

# GENESPACE: syntenic pan-genome annotations for eukaryotes

John T. Lovell<sup>\*1,2</sup>, Avinash Sreedasyam<sup>1</sup>, M. Eric Schranz<sup>3</sup>, Melissa A. Wilson<sup>4</sup>, Joseph W. Carlson<sup>2</sup>, Alex Harkess<sup>1,5</sup>, David Emms<sup>6</sup>, David Goodstein<sup>2</sup>, Jeremy Schmutz<sup>1,2</sup>

<sup>1</sup>Genome Sequencing Center, HudsonAlpha Institute for Biotechnology, Huntsville, AL, USA

<sup>2</sup>Joint Genome Institute, Lawrence Berkeley National Laboratory, Berkeley, CA, USA

<sup>3</sup>Biosystematics Group, Wageningen University and Research, Wageningen, The Netherlands

<sup>4</sup>Center for Evolution and Medicine, School of Life Sciences, Arizona State University, Tempe, AZ, USA

<sup>5</sup>Department of Crop, Soil, and Environmental Sciences, Auburn University, Auburn, AL, USA

<sup>6</sup>Oxford University, Oxford, United Kingdom

\*Corresponding author, email: [jlovell@hudsonalpha.org](mailto:jlovell@hudsonalpha.org)

The development of multiple high-quality reference genome sequences in many taxonomic groups has yielded a high-resolution view of the patterns and processes of molecular evolution. Nonetheless, leveraging information across multiple reference haplotypes remains a significant challenge in nearly all eukaryotic systems. These challenges range from studying the evolution of chromosome structure, to finding candidate genes for quantitative trait loci, to testing hypotheses about speciation and adaptation in nature. Here, we address these challenges through the concept of a pan-genome annotation, where conserved gene order is used to restrict gene families and define the expected physical position of all genes that share a common ancestor among multiple genome annotations. By leveraging pan-genome annotations and exploring the underlying syntenic relationships among genomes, we dissect presence-absence and structural variation at four levels of biological organization: among three tetraploid cotton species, across 300 million years of vertebrate sex chromosome evolution, across the diversity of the Poaceae (grass) plant family, and among 26 maize cultivars. The methods to build and visualize syntenic pan-genome annotations in the GENESPACE R package offer a significant addition to existing gene family and synteny programs, especially in polyploid, outbred and other complex genomes.

## INTRODUCTION

De novo genome assemblies and gene model annotations represent increasingly common resources that describe the sequence and putative functions of protein coding and intergenic regions within a single genotype. Evolutionary relationships among these DNA sequences are the foundation of many molecular tools in modern medical, breeding and evolutionary biology research. Perhaps the most crucial inference to make when comparing genomes revolves around homologous genes, which share an evolutionary common ancestor and ensuing sequence or protein structure similarity. Analyses of homologs, including comparative gene expression, epigenetics, and sequence evolution, require the distinction between orthologs which arise from speciation events, and paralogs, which arise from sequence duplications. In some systems, this is a simple task where most genes are single copy, and orthologs are synonymous with reciprocal best-scoring BLAST hits. Other sequence similarity approaches such as OrthoFinder (1, 2) leverage graphs and gene trees to test for orthology, permitting more robust analyses in systems with gene copy number (CNV) or presence-absence variation (PAV). However, whole-genome duplications (WGDs), chromosomal deletions, and variable rates of sequence evolution, such as sub-genome dominance in polyploids, can confound the evidence of orthology from sequence similarity alone.

The physical position of homologs offers a second line of evidence that can help to overcome challenges posed by WGDs, tandem arrays, heterozygous-duplicated regions, and other genomic complexities (3–5). Synteny, or the conserved order of DNA sequences among chromosomes that share a common ancestor, is a typical feature of eukaryotic genomes. In some taxa, synteny is preserved across hundreds of millions of years of evolution and is retained over multiple whole genome duplications (6–8). Such signals of evolutionary coalescence are often lost in DNA sequences of protein coding genes. Like chromosomal scale synteny, conserved gene order collinearity along local regions of chromosomes can provide evidence of homology, and in some cases enable determinations of whether two regions diverged as a result of speciation or a large scale duplication event (5). Combined, evidence of gene collinearity and sequence similarity should improve the ability to classify paralogous and orthologous relationships beyond either approach in isolation.

Integrating synteny and collinearity into comparative genomics pipelines also physically anchors the positions of related gene sequences onto the assemblies of each genome. For example, by exploring only syntenic orthologs it is possible to examine all putatively functional variants within a genomic region of interest, even those that are absent in the focal reference genome (9). Such a pan-genome annotation framework (10) would permit easy access to multi-genome networks of high-confidence

58 orthologs and paralogs, regardless of ploidy or other  
59 complicating aspects of genome biology. Here, we present  
60 GENESPACE, an analytical pipeline (Supplemental Fig. 1)  
61 that explicitly links synteny and sequence similarity to  
62 provide high-confidence inference about networks of  
63 genes that share a common ancestor, and represents  
64 these networks as a pan-genome annotation. We then  
65 leverage this framework to explore gene family evolution in  
66 flowering plants, mammals and reptiles.

## RESULTS AND DISCUSSION

### GENESPACE methods to compare multiple complex genomes

72 Until recently, most genome assemblies were haploid,  
73 representing meiotically homologous chromosomes as a  
74 single haplotype. While this is certainly appropriate for  
75 inbred or haploid species, such a representation does not  
76 adequately address heterozygosity in outbred species or  
77 homeologous chromosomes, which have diverged  
78 following a whole-genome duplication in polyploid  
79 genomes. With the advent of accurate long-read  
80 sequencing, many state-of-the-art genomes of diploid  
81 eukaryotes are now phased, representing both  
82 homologous chromosomes in the assembly (10, 11). The  
83 representation of both meiotically homologous  
84 chromosomes in outbred diploids introduces a problem  
85 well known in polyploid comparative genomics: paralogs,  
86 which are duplicated within a genome, such as homeologs  
87 in polyploids or meiotic homologs in outbred diploid  
88 genomes, are not as accurately inferred as single-copy  
89 orthologs among genomes by graph-based clustering  
90 programs. This challenge can be easily addressed in  
91 genomes with two complete and easily identifiable sub-  
92 genomes (or alternative haplotypes) by splitting  
93 chromosomes into separate haploid genomes. However,  
94 this splitting approach is not possible in many outbred or  
95 polyploid genomes due to chromosomal rearrangements  
96 (e.g. maize, see below), and segmental duplications or  
97 deletions (e.g. sex chromosomes, see below). Given these  
98 known biases, it is crucial to develop a comparative  
99 genomics framework that performs adequately in outbred  
100 and polyploid genomes.

101 GENESPACE overcomes the challenge of accurately  
102 finding homeologous or meiotically homologous gene pairs  
103 by constraining orthogroups (OGs) within synteny regions.  
104 In short, GENESPACE subsets raw global OrthoFinder

105 OGs to synteny by dropping graph edges that span non-  
106 syntenic genomic coordinates, thus producing split  
107 synteny-constrained OG subgraphs (Supplemental Fig. 1).  
108 GENESPACE can then run Orthofinder on BLAST hits  
109 within syntenic regions which, when merged with synteny-  
110 constrained OGs, produces within-block OGs. Within-  
111 block graphs can better capture subgraphs containing  
112 distant paralogs because hit scores outside of the focal  
113 region are not considered, thereby effectively inferring  
114 paralogs with similar efficacy to orthologs (Table 1).  
115 GENESPACE then projects the syntenic position of each  
116 orthogroup against a single genome assembly of any  
117 ploidy, which permits representation of gene presence-  
118 absence (PAV) and copy-number (CNV) variation as  
119 physically anchored subgraphs along the reference  
120 genome. We term this resource a ‘pan-genome  
121 annotation’. Since analyses are conducted within syntenic  
122 regions, GENESPACE is agnostic to ploidy, duplicated or  
123 deleted regions, inversions, or other common  
124 chromosomal complexities.

125 As a proof of concept, we compared the GENESPACE  
126 synteny-constrained orthology inference method with  
127 global and sub-genome split OrthoFinder runs using three  
128 allotetraploid cotton genomes (12). These genomes offer  
129 an ideal system to test orthology inference methods due to  
130 their easily identifiable sub-genomes, which resulted from  
131 an ancient 1.0-1.6 million (M) year ago (ya) whole-genome  
132 duplication (WGD), and significant molecular divergence  
133 among genomes (160-630k ya). To determine the  
134 sensitivity of each approach, we calculated the percent of  
135 genes or tandem array representatives captured in  
136 orthogroups that were placed in exactly one syntenic  
137 position on each sub-genome (Supplemental Fig. 2). Given  
138 the known high degree of sequence conservation and little  
139 gene presence-absence variation among these cotton  
140 genomes and sub-genomes (12), most orthogroups should  
141 have six syntenic positions across the three cotton  
142 genomes, each with two sub-genomes. Therefore, the  
143 most accurate method should produce more single-copy  
144 orthogroups with exactly six syntenic positions. Given this  
145 metric, the run where the sub-genomes were split into  
146 separate “species” outperformed the tetraploid run,  
147 recovering 9% more orthogroups present only on  
148 homologous or homeologous chromosomes across all six  
149 sub-genomes. However, GENESPACE’s method to re-run  
150 OrthoFinder on synteny constrained within-block BLAST  
151 hits effectively brought genome-wide single-copy

**Table 1 | Summary of orthogroup (‘OG’) inference for polyploids.**

Orthofinder was run using default settings on three tetraploid inbred cotton genomes (represented as diploid assemblies) and six split sub-genomes. Counts of single-copy orthogroups (more = better) are presented for nine cotton chromosomes.

	tetraploid	split by subg.	% split better
n. *global 1x/homeolog OGs	-- 15,280	16,804	9.1%
n. **synteny-constr. 1x OGs	-- 18,433	21,317	13.5%
n. ***within-block 1x OGs	-- 21,989	21,652	-1.6%

\*‘Global’ orthogroups were parsed directly from the raw orthofinder (-og) run.

\*\*Synteny-constrained orthogroups are split so that only graph edges within synteny regions between (sub)genomes are retained. \*\*\*Within block orthogroups are re-calculated from BLAST hits within pairwise synteny regions.

**Table 2 | Summary of synteny blocks between *G. barbadense* sub-genomes.** MCScanX\_h was run for each subset of BLAST hits and the copy number of each non-overlapping 10kb genomic interval was tabulated from the start/end coordinates of the unique blocks from the collinearity file. The percent of 10kb intervals that are never found within a block (absent), found within exactly one block (single-copy) or in more than one block (multi-copy) are reported.

	% absent <sup>+</sup>	% single-copy <sup>+</sup>	% multi-copy <sup>+</sup>
Raw BLAST hits	-- 6.5	79.5	14.0
Collinear array reps.	-- 6.1	83.1	10.7
OG-constrained	-- 6.1	91.3	2.6
*GENESPACE default	-- 5.6	93.7	0.6

<sup>+</sup>The GENESPACE-calculated block coordinates, which uses MCScanX.

<sup>+</sup>global % of 10kb intervals in each category.

152 orthogroup inference in line with the sub-genome split  
153 methods (Table 1). These results indicate that, in contrast  
154 to previous approaches, GENESPACE infers homeologs  
155 between polyploid sub-genomes with similar precision as  
156 orthologs among haploid genomes.

157 In addition to improved accuracy and precision of  
158 syntenic orthogroup inference, GENESPACE's method to  
159 find syntenic regions and blocks outperforms collinearity  
160 estimates from the program MCScanX (4), which serves as  
161 an important tool for synteny inference (Table 2). To  
162 demonstrate this improvement, we contrasted the two  
163 sub-genomes of 'Pima' cotton (*Gossypium barbadense*).  
164 The 1-1.6M ya divergence between these sub-genomes  
165 resulted in many minor and several major inversions and  
166 translocations (Supplemental Fig. 2), yet the two genomes  
167 remain nearly completely intact and single-copy, excluding  
168 tandem arrays. Thus, the vast majority of each sub-  
169 genome should correspond to exactly one position in the  
170 alternative sub-genome. To test the performance of  
171 syntenic block calculations, we tabulated the proportion of  
172 10kb genomic intervals in the expected single-copy  
173 dosage or likely erroneous (absent or multi-copy) copy  
174 number for three different BLAST hit subsets piped into  
175 MCScanX and the complete GENESPACE method (Table  
176 2). MCScanX's sensitivity causes non-orthologous blocks  
177 and overlapping block breakpoints to be included at a high

178 rate: 14% of all intervals were multi-copy in the MCScanX  
179 run using raw BLAST hits. However, this issue can be  
180 partially resolved by subsetting the BLAST hits to those  
181 within the same orthogroups (2.6% multi-copy). This  
182 orthogroup constraint performance improvement is the  
183 major motivator for the GENESPACE synteny pipeline,  
184 which uses orthogroup-constrained BLAST hits as the  
185 initial seed for syntenic blocks, then searches all hits within  
186 a fixed radius to these anchors. This second proximity  
187 search step also resulted in significant gains in single-copy  
188 syntenic regions between sub-genomes, simultaneously  
189 reducing the amount of un-represented (6.1% to 5.6%) and  
190 multi-copy (2.6% to 0.6%) sequences. Combined, these  
191 results demonstrate a marked improvement in synteny  
192 discovery and block coordinate assignment.

#### 193 194 Synteny-anchored vertebrate sex chromosomes pan- 195 genome annotations

196 The GENESPACE pan-genome annotation facilitates  
197 the exploration and analysis of sequence evolution across  
198 multiple genomes within regions of interest (ROI). Some  
199 common use applications include the analysis of QTL  
200 intervals (see the next section), or tests of genome  
201 evolution at larger phylogenetic scales. One particularly  
202 instructive example comes from the origin and evolution of  
203 the mammalian XY and avian ZW sex chromosome

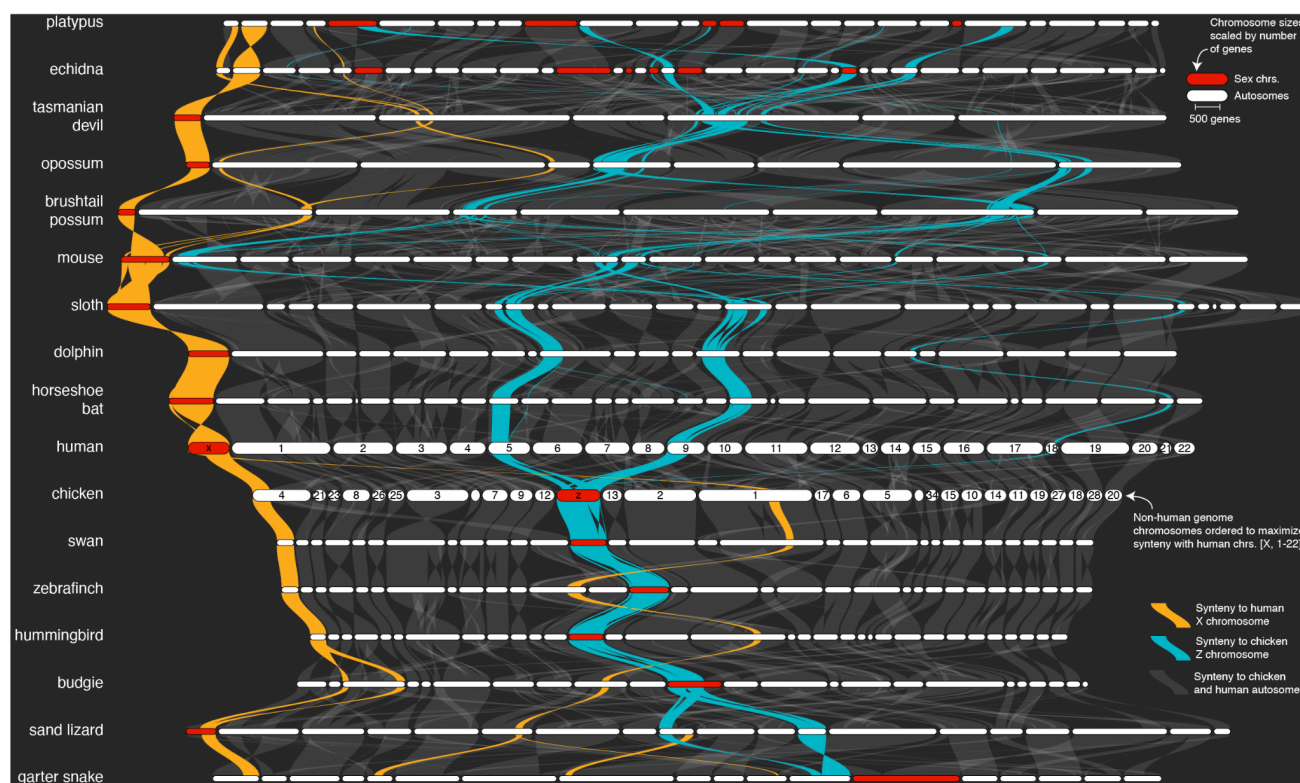


**Fig. 1 | Structural evolution of mammalian X and avian Z sex chromosomes.** The reptilian, avian, and mammalian sex chromosomes synteny network across 17 representative vertebrate genomes (two reptile, five eutherian mammal, three marsupial, two monotreme, and five avian genomes; see Supplemental Fig. 3 for the full synteny graph including autosomes and chromosome labels). The plot was generated by the GENESPACE function plot\_riparian. Genomes are ordered vertically to maximize synteny between sequential pairwise genomes. Chromosomes are ordered horizontally to maximize synteny with the human chromosomes [X, Y, 1-22]. Regions containing syntenic orthogroup members to the mammalian X (gold) or avian Z (blue) chromosomes are highlighted. All sex chromosomes are represented by red segments (except the bat chr1, which is most likely the X chromosome but is not represented as such in the assembly), while autosomes are white. Chromosomes are scaled by the total number of genes in synteny networks and positions of the braids are the gene order along the chromosome sequence.

systems. To explore these chromosomes, we ran GENESPACE on 15 haploid avian and mammalian genome assemblies (Table 3), spanning most major clades of birds, placental mammals, monotremes and marsupials with chromosome-scale annotated reference genomes (Supplemental Fig. 3, Supplemental Data 1-2). We also included two reptile genomes as outgroups to the avian genomes. The heteromorphic chromosomes (Y and W) are often un-assembled, or, where assemblies exist, lack sufficient synteny to provide a useful metric for comparative genomics. As such, we chose to focus on the homomorphic X and Z chromosomes, which have remained surprisingly intact over the >100M years of independent mammalian (13) and avian evolution (14) (Fig. 1).

While the same or similar genomic regions often recurrently evolve into sex chromosomes, perhaps due to ancestral gene functions involved in gonadogenesis, evidence about the non-randomness of sex chromosome evolution is still contentious (15). Given our analysis, it is clear that the avian Z chromosome did not evolve from either of the two reptile Z chromosomes sampled here, but instead likely arose from autosomal regions or unsampled ancestral sex chromosomes. The situation in mammals is less clear, in part because both reptile genomes are more closely related to avian than mammalian genomes, which makes ancestral state reconstructions between the two groups less accurate. Nonetheless, the mammalian X and sand lizard Z chromosomes partially share synteny orthology, an outcome that would be consistent with common descent from a shared ancestral sex chromosome or autosome containing sex-related genes. The shared 91.7M bp region between the human X and sand lizard Z represents 59.0% of the human X chromosome genic sequence. The remaining 64.0M bp of human X linked sequence are syntenic with autosomes 4 (9.9M bp) and 16 (119.6M bp) in sand lizard. The same region is syntenic across three autosomes in the garter snake genome (Fig. 1, Supplemental Data 3).

The eutherian mammalian X chromosome is largely composed of two regions, an X-conserved ancestral sex chromosome region that arose in the common ancestor of therian mammals, and an X-added region that arose in the common ancestor of eutherians (16). Consistent with this evolutionary history, the X chromosome is syntenic across all five eutherian mammals studied here. Further, a 107.2M bp (68.8%) segment of the human X, which corresponds with the X-conserved region, is syntenic with 77.8M bp (93.9%) of the tasmanian devil X chromosome and represents the entire syntenic region between the human and all three marsupial X chromosomes (Fig. 1).

Similarly, the chicken Z chromosome is retained in its entirety across all five avian genomes. The only notable exception being the budgie Z chromosome, which also features a partial fusion between the Z and an otherwise autosomal 19.5M bp segment of chicken chromosome 11 (Fig. 1, Supplemental Data 3), potentially representing a neo-sex chromosome fusion that has not yet been described.

In contrast to conserved eutherian and avian sex chromosomes, the complex monotreme  $X_nY_n$  sex chromosomes are only partially syntenic between the two sampled genomes. Only the first X chromosomes are ancestral to both echidna and platypus (17), and all are unrelated to the mammalian X chromosomes (Fig. 1, Supplemental Fig. 3), consistent with their independent evolution (17). Interestingly, the entirety of the echidna X4 and 47.6M bp (67.9%) of the genic region of the platypus X5 chromosomes are syntenic with the avian Z chromosome (Fig. 1). The phylogenetic scale of the genomes presented here precludes evolutionary inference about the origin of these shared sex chromosome sequences; however, the possibility of parallel evolution of sex chromosomes between such diverged lineages may prove an interesting future line of inquiry.

### Exploiting synteny to track candidate genes in grasses

The Poaceae grass plant family is one of the best studied lineages of all multicellular eukaryotes and includes experimental model species (*Brachypodium distachyon*; *Panicum hallii*; *Setaria viridis*) and many of the most productive (*Zea mays* - maize/corn; *Triticum aestivum* - wheat, *Oryza sativa* - rice) and emerging (*Sorghum bicolor* - sorghum; *P. virgatum* - switchgrass) agricultural crops. Despite the tremendous genetic resources of these and other grasses, genomic comparisons among grasses are difficult, in part because of an ancient polyploid origin (see the next section), and because subsequent whole-genome duplications are a feature of most clades of grasses. For example, maize is an 11.4M ya paleo-polyploid (18), allo-tetraploid switchgrass formed 4-6M ya (19), and allo-hexaploid bread wheat arose about 8k ya (20). In some cases, homeologous gene duplications from polyploidy have generated genetic diversity that can be targeted for crop improvement; however, in other cases the genetic basis of trait variation may be restricted to sequences that arose in a single sub-genome. Thus, it is crucial to contextualize comparative-quantitative genomics searches and explicitly explore only the orthologous or homeologous regions of interest when searching for markers or candidate genes underlying heritable trait variation — a significant challenge in the complex and polyploid grass genomes. To help overcome this challenge and provide tools for grass comparative genomics, we conducted a GENESPACE run and built an interactive viewer hosted on Phytozome (21) among genome annotations for the eight grass species listed above. Owing to its use of within-block orthology and synteny constraints, GENESPACE is ideally suited to conduct comparisons across species with diverse polyploidy events. Default parameters produced a largely contiguous map of synteny even across notoriously difficult comparisons like the paleo homeologs between the maize sub-genomes (Fig. 2a, Supplemental Fig. 4, Supplemental Data 4). Furthermore, the sensitive synteny construction pipeline implemented by GENESPACE effectively masks additional paralogous regions like those from the *Rho*

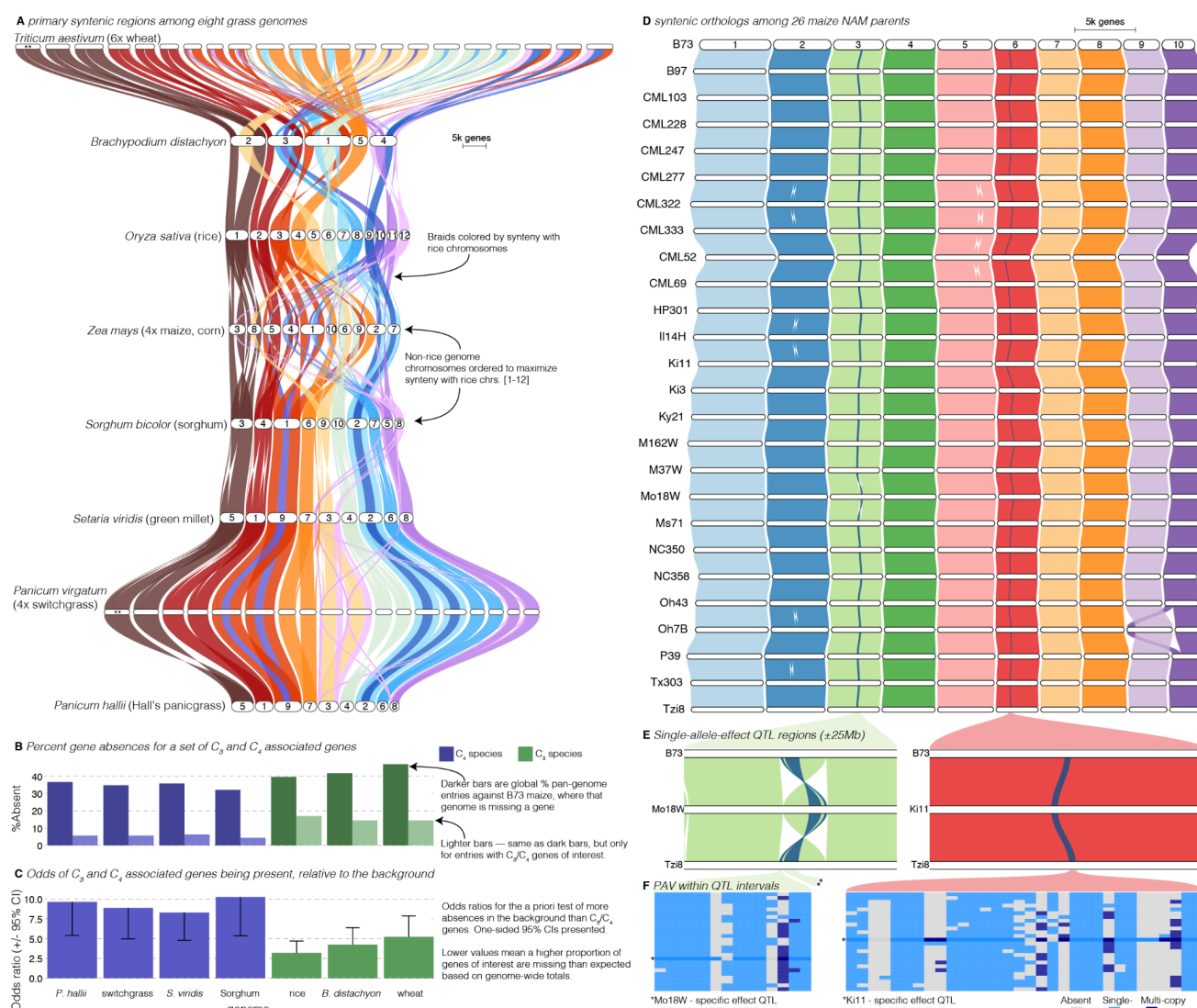


**Fig. 2 | Comparative-quantitative genomics in the grasses.** **A** The GENESPACE synteny map ('riparian plot') of orthologous regions among eight grass genomes. Chromosomes are ordered to maximize synteny with rice and ribbons are color-coded by synteny to rice chromosomes. Chromosome names are too long to fit for the neo-polyploids (\*\*); Supplemental Figure 4 contains names of all chromosomes. **B** The upper bars display the proportion of maize gene models without syntenic orthologs ("absent") in each genome, split by the full background (dark colors) and 86 genes annotated for roles in the evolution of  $C_3/C_4$  photosynthesis. **C** The proportion of absent genes is higher in the  $C_3$  genomes (green bars), even when controlling for more global gene absences (lower odds ratios). **D** Syntenic orthologs, controlling for homologs among the 26 maize NAM founder genomes, with two general QTL intervals highlighted. **E** Focal QTL regions that affect productivity in drought where only the genome that drives the QTL effect (middle genome); the top (B73) and bottom (Tz18) genomes are presented and the region plotted is restricted to the 50Mb physical B73 interval surrounding the QTL. Note that the chr3 QTL disarticulates into two intervals. Due to a larger number of potential candidate genes, the larger chr3 region, flagged with \*\*, is explored separately in Supplemental Figure 6. **F** Presence-absence and copy number variation are presented for two of the three intervals. The focal genome is flagged \* and its corresponding map colors are more saturated.

321 duplication that gave rise to all extant grasses (but see 333 under forecasted increased heat load of the next century. 322 below).

323 Breeders and molecular biologists can take two general 333 approaches to understanding the genetic basis of complex 334 traits: studying variation caused by *a priori*-defined genes 335 of interest, or determining candidate genes from genomic 336 regions of interest. As an example of the exploration of lists 337 of *a priori*-defined candidate genes, we analyzed the 338 functional and presence-absence variation of 86 genes 339 shown to be involved in the transition between  $C_3$  and  $C_4$  340 photosynthesis (22), the latter permitting ecological 341 dominance in arid climates and agricultural productivity 342

343 344 To conduct this analysis, we built pan-genome annotations 345 across the seven grasses anchored to  $C_4$  maize 346 (Supplemental Data 5), which was the genome in which 347 these genes were discovered. This resulted in 159 pan- 348 genome entries; nearly always two placements for each 349 gene in the paleo-tetraploid maize genome. Given that 350 many of these genes were discovered in part because of 351 sequence similarity to genes in *Arabidopsis* and other 352 diverged plant species, it is not surprising that PAV among 353  $C_3/C_4$  genes was lower than the background (9.7% vs 354 38.2%, odds = 5.7,  $P < 1 \times 10^{-16}$ ; Fig. 2b). However, these

345 ratios were highly variable among genomes, particularly 405 genome (Fig. 3d-e). Since inversions reduce  
346 among the C<sub>3</sub> species (wheat, rice, *B. distachyon*), which 406 recombination, it is possible that multiple Mo18W causal  
347 had far higher percent absences than the C<sub>4</sub> species 407 variants have been fixed in linkage disequilibrium in this  
348 (15.3% vs. 5.5%, odds = 3.1, P = 6.25x10<sup>-8</sup>, Fig. 2b). This 408 NAM population. In addition to this chromosomal mutation  
349 effect is undoubtedly due in part to the increased 409 and sequence variation between the parents and B73 (23),  
350 evolutionary distance between maize and the C<sub>3</sub> species 410 we sought to define additional candidate genes from the  
351 compared to the other C<sub>4</sub> species. However, when 411 patterns of presence-absence and copy-number variation,  
352 controlling for the elevated level of absent genes globally 412 explicitly looking for genes that were private to the focal  
353 in C<sub>3</sub> species, the effect was still very strong: the odds of 413 genome. Two genes in the smaller chr3 and one gene in  
354 C<sub>3</sub> species having more of these C<sub>3</sub>/C<sub>4</sub> genes at syntenic 414 the larger chr3 interval were private to Mo18W and four  
355 pan-genome positions than the background was always 415 genes in three pangenome entries (one two-member array)  
356 lower than the C<sub>4</sub> species (Fig. 2c). Despite these 416 were private to Ki11 in the chr6 interval (Fig. 2f,  
357 interesting patterns, given only a single C<sub>3</sub>/C<sub>4</sub> phylogenetic 417 Supplemental Fig. 6, Supplemental Data 7). While none of  
358 split in this dataset, it is impossible to test evolutionary 418 these genes have functional annotations relating to  
359 hypotheses regarding the causes of such PAV. 419 drought, this method provides additional candidates that  
360 Nonetheless, this result suggests a possible role of gene 420 would not have been discovered by B73-only candidate  
361 loss or gain as an evolutionary mechanism for drought- and 421 gene exploration.

362 Like the exploration of *a priori*-defined sets of genes, 422  
363 finding candidate genes within quantitative trait loci (QTL) 423 **Studying the whole-genome duplication that led to the**  
364 intervals usually involves querying a single reference 424 **diversification of the grasses**  
365 genome and extracting genes with promising annotations 425 Like most plant families (25–27), but unlike nearly all  
366 or putatively functional polymorphism. In the case of a 426 animal lineages (28), the grasses radiated following a  
367 biparental mapping population genotyped against a single 427 whole-genome duplication: the ~70M ya *Rho* WGD. The  
368 reference, this is a fairly trivial process where genes within 428 resulting gene family redundancy and gene-function sub-  
369 physical bounds of a QTL are the candidates. However, 429 functionalization is hypothesized to underlie the  
370 many genetic mapping populations now have reference 430 tremendous ecological and morphological diversity of  
371 genome sequences for all parents; this offers an 431 grasses (29–31). To explore sequence variation among  
372 opportunity to explore variation among functional alleles 432 *Rho*-derived paralogs, we used GENESPACE to build a  
373 and presence absence variation, which would be 433 ploidy-aware syntenic pan-genome annotation among  
374 impossible with a single reference genome. GENESPACE 434 these eight species (Supplemental Data 8), using the built-  
375 is ideally suited for this type of exploration, and indeed was 435 in functionality that allows the user to mask primary (likely  
376 originally designed to solve this problem between the two 436 orthologous) syntenic regions and search for secondary  
377 *P. hallii* reference genomes and their F<sub>2</sub> progeny (9) using 437 hits (likely paralogous, Fig. 3a). Overall, the peptide identity  
378 synteny to project the positions of genes across multiple 438 between *Rho*-derived paralogous regions was much lower  
379 genomes onto the physical positions of a reference. 439 than orthologs among species (e.g. *S. viridis* vs. *P. hallii*:  
380 Wilcoxon W = 88094632, P < 10<sup>-16</sup>; Supplemental Data 9),  
381 To illustrate this approach, we re-analyzed QTL 440 consistent with the previous discovery that the *Rho*  
382 generated from the 26-parent USA maize nested 441 duplication predated the split among most extant grasses  
383 association mapping (NAM) population (23). Originally, 442 by >20M years (32). However, as has been previously  
384 candidates for these QTL were defined by the proximate 443 observed, there is significant variation in the relative  
385 gene models only in the B73 reference genome (23); 444 similarity of *Rho*-duplicated chromosome pairs (33). As an  
386 however, with GENESPACE and the recently released 445 example, the peptide sequences of single-copy gene hits  
387 NAM parent genomes (24), it is now possible to evaluate 446 in primary syntenic regions (median identity = 90.6%)  
388 candidate genes present in the genomes of other NAM 447 between chromosome 8 of *P. hallii* and *S. viridis*, were  
389 founder lines but either absent or unannotated in the B73 448 26.9% more similar than the secondary *Rho*-derived  
390 reference genome. We built a single-copy synteny graph of 449 regions (median identity = 71.4%, Wilcoxon W = 87842, P  
391 all 26 NAM founders, anchored to the B73 genome to 450 < 10<sup>-16</sup>). However, *S. viridis* chromosome 8 contained a  
392 explore this possibility (Fig. 2d; Supplemental Data 6; 451 single paralogous region between all seven grass genomes  
393 Supplemental Fig. 5) and extracted the three QTL intervals 452 that could not be distinguished from the primary regions,  
394 (Fig. 2d-e) where the allelic effect of a single parental 453 based on synteny or orthogroup identity. Unlike all other  
395 genome was an outlier relative to all other alleles. Such 454 *Rho*-derived blocks, the *P. hallii* paralogs to this 2.7M bp  
396 ‘private’ allelic contributions, which may be driven by 455 chromosome 8 region were not significantly less conserved  
397 parent-specific sequence variation, were manifest here as 456 than the primary orthologous region (91.6% vs. 91.9%, W  
398 delayed period of silking-anthesis of progeny with the 457 = 14830, P = 0.13). Outside of this region, the peptide  
399 Mo18W allele at two adjacent Chr3 QTLs and reduced 458 identity of paralogs dropped back to the genome-wide  
400 plant height under drought for progeny with the Ki11 allele 459 average (Fig. 3b).

401 Indeed, the GENESPACE run treating the eight 460  
402 genomes as haploid representations could not distinguish 461 between the *Rho* derived paralogs in the over-retained  
403 to find that the two Mo18W QTL regions exist within a 462  
404 11.7M bp derived inversion that is only found in the Mo18W 463

405 genome (Fig. 3d-e). Since inversions reduce 406 recombination, it is possible that multiple Mo18W causal  
407 variants have been fixed in linkage disequilibrium in this  
408 NAM population. In addition to this chromosomal mutation  
409 and sequence variation between the parents and B73 (23),  
410 we sought to define additional candidate genes from the  
411 patterns of presence-absence and copy-number variation,  
412 explicitly looking for genes that were private to the focal  
413 genome. Two genes in the smaller chr3 and one gene in  
414 the larger chr3 interval were private to Mo18W and four  
415 genes in three pangenome entries (one two-member array)  
416 were private to Ki11 in the chr6 interval (Fig. 2f,  
417 Supplemental Fig. 6, Supplemental Data 7). While none of  
418 these genes have functional annotations relating to  
419 drought, this method provides additional candidates that  
420 would not have been discovered by B73-only candidate  
421 gene exploration.

422  
423 **Studying the whole-genome duplication that led to the**  
424 **diversification of the grasses**  
425 Like most plant families (25–27), but unlike nearly all  
426 animal lineages (28), the grasses radiated following a  
427 whole-genome duplication: the ~70M ya *Rho* WGD. The  
428 resulting gene family redundancy and gene-function sub-  
429 functionalization is hypothesized to underlie the  
430 tremendous ecological and morphological diversity of  
431 grasses (29–31). To explore sequence variation among  
432 *Rho*-derived paralogs, we used GENESPACE to build a  
433 ploidy-aware syntenic pan-genome annotation among  
434 these eight species (Supplemental Data 8), using the built-  
435 in functionality that allows the user to mask primary (likely  
436 orthologous) syntenic regions and search for secondary  
437 hits (likely paralogous, Fig. 3a). Overall, the peptide identity  
438 between *Rho*-derived paralogous regions was much lower  
439 than orthologs among species (e.g. *S. viridis* vs. *P. hallii*:  
440 Wilcoxon W = 88094632, P < 10<sup>-16</sup>; Supplemental Data 9),  
441 consistent with the previous discovery that the *Rho*  
442 duplication predated the split among most extant grasses  
443 by >20M years (32). However, as has been previously  
444 observed, there is significant variation in the relative  
445 similarity of *Rho*-duplicated chromosome pairs (33). As an  
446 example, the peptide sequences of single-copy gene hits  
447 in primary syntenic regions (median identity = 90.6%)  
448 between chromosome 8 of *P. hallii* and *S. viridis*, were  
449 26.9% more similar than the secondary *Rho*-derived  
450 regions (median identity = 71.4%, Wilcoxon W = 87842, P  
451 < 10<sup>-16</sup>). However, *S. viridis* chromosome 8 contained a  
452 single paralogous region between all seven grass genomes  
453 that could not be distinguished from the primary regions,  
454 based on synteny or orthogroup identity. Unlike all other  
455 *Rho*-derived blocks, the *P. hallii* paralogs to this 2.7M bp  
456 chromosome 8 region were not significantly less conserved  
457 than the primary orthologous region (91.6% vs. 91.9%, W  
458 = 14830, P = 0.13). Outside of this region, the peptide  
459 identity of paralogs dropped back to the genome-wide  
460 average (Fig. 3b).

461 Indeed, the GENESPACE run treating the eight  
462 genomes as haploid representations could not distinguish  
463 between the *Rho* derived paralogs in the over-retained

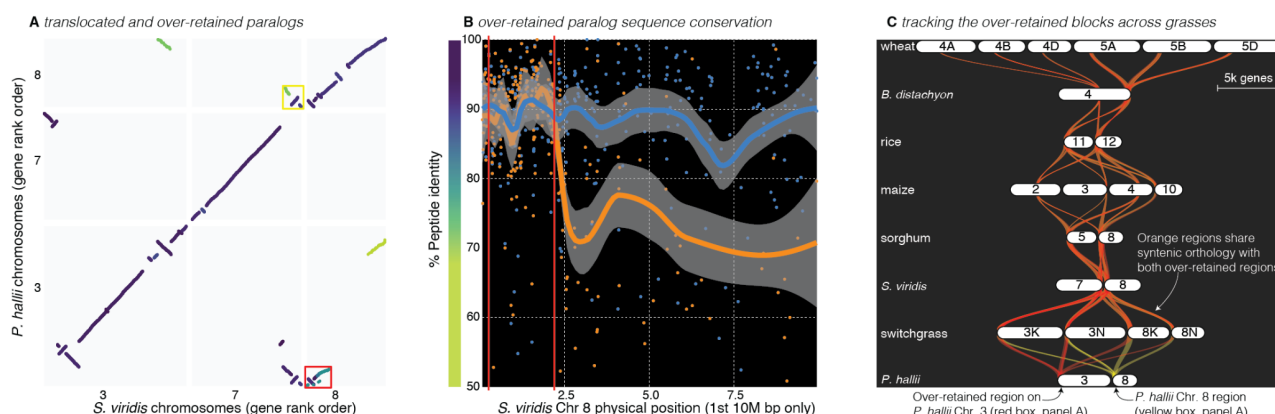


**Fig. 3 | Analysis of the grass Rho WGD.** **A** Syntenic anchor blast hits where the target and query genes were in the same orthogroup between *P. hallii* and *S. viridis* genomes. The color of each point indicates the peptide identity of each pair of sequences; the color scale is shown along the y axis of panel B. **B** The protein identity of *S. viridis* chromosome 8 primary orthologous (blue line) hits against *P. hallii* chromosome 8 and the secondary hits (orange line) against *P. hallii* chromosome 3 demonstrate sequence conservation heterogeneity. The region between the two red vertical lines corresponds to the red-boxed over-retained primary block in panel A. **C** The two boxed regions in panel A were tracked from their origin on *P. hallii* chromosome 3 (red) and 8 (yellow). Note that all syntenic orthologous regions across the graph contain both *P. hallii* source regions (50% transparency of the braids - overlapping regions appear orange).

region across all grasses (Fig. 3c), with the exception of all chromosome pairs between *B. distachyon* and wheat and blocks connecting Maize chromosome 10 to sorghum chromosome 5. It is interesting to note that all syntenic over-retained regions are at the extreme terminus of the chromosomes outside of maize, *B. distachyon* and wheat; further, the only genome with complete segregation of the two paralogs, wheat, also retains these regions in the center of all six chromosomes (Fig. 3c). These results are consistent with the proposed evolutionary mechanism (33) where concerted evolution and “illegitimate” homeologous recombination may have homogenized these paralogous regions. This process would be less effective in pericentromeric regions than the chromosome tails, where a single crossover event would be sufficient to homogenize two paralogous regions that arose 70M ya.

## Conclusions

Combined, the historical abundance of genetic mapping studies and ongoing proliferation of genome resources provides a strong foundation for the integration of comparative and quantitative genomics to accelerate discoveries in evolutionary biology, medicine, and agriculture. The incorporation of synteny and orthology into comparative genomics and quantitative genetics pipelines offers a mechanism to bridge these disparate disciplines. Here, we presented the GENESPACE R package and the syntenic pan-genome annotation as a framework to help bridge the current gaps between comparative and quantitative genomics, especially in complex evolutionary systems. We hope that the examples presented here will inspire further work to leverage the powerful genome-wide annotations that are coming online, both within and among species.

## METHODS

All analyses were performed in R 4.1.2 on macOS Big Sur 10.16. The following R packages were used either for visualization or within GENESPACE v0.9.3 (11-February 2022 release): data.table v1.14.0

503 (42), dbscan v1.1-8 (43), igraph v1.2.6 (44), Biostrings v2.58.0 (45),  
 504 rtracklayer v1.50.0 (46). GENESPACE also calls the following third  
 505 party software: diamond v2.0.8.146 (47), OrthoFinder v2.5.4 (7), and  
 506 MCScanX no version installed on 10/23/2020 (4).

507 All results, tables (except Table 3), figures (except Fig. S1) and  
 508 statistics were generated programmatically; the accompanying scripts  
 509 and key output are available on github: [jtlovell/GENESPACE\\_data](https://github.com/jtlovell/GENESPACE_data).  
 510 Minor adjustments to figures to improve clarity were accomplished in  
 511 Adobe Illustrator v26.01. Below, we provide a high-level description of  
 512 the GENESPACE pipeline and the methods to produce the results  
 513 presented here. A full description of each step in GENESPACE is  
 514 provided in the documentation that accompanies the package source  
 515 code on github ([jtlovell/GENESPACE](https://github.com/jtlovell/GENESPACE)).

516

## Description of the vignettes

517 Raw genome annotations were downloaded on or before 8-  
 518 October 2021. See Table 3 for data sources, citations and metadata.  
 519 For the analyses presented here, we conducted six GENESPACE runs:  
 520 cotton tetraploid, cotton sub-genome-split, vertebrates, grasses,  
 521 grass Rho duplication, and maize 26 NAM parents.

522 All GENESPACE runs used default parameterization, with the  
 523 following exceptions: (1) both cotton runs used a minimum block size  
 524 and maximum number of gaps of 10 (default = 5 for both), (2) the Rho  
 525 grass run allowed a single secondary hit (default is 0, this is how the  
 526 paralogs are explicitly searched for) and maximum number of gaps in  
 527 secondary regions of 10 (default is 5, relaxed to reduce ancient  
 528 paralogous block splitting), and (3) the maize run used the “fast”  
 529 OrthoFinder method since all genomes are closely related and haploid.  
 530 Some maize genomes contain small alternative haplotype scaffolds,  
 531 which were dropped for all analyses.

532 The cotton runs employed the GENESPACE “outgroup”  
 533 functionality, which allows the user to specify a genome that is  
 534 included in the seed OrthoFinder run, but is ignored for all synteny and  
 535 pan-genome construction steps. This can be important when dealing  
 536 with highly diverged species that do not share complete synteny, but  
 537 are needed for accurate orthogroup inference. For example, a run with  
 538 only the three cotton genomes would be likely to split sub-genome  
 539 orthogroups since the WGD predated speciation. As such, we included  
 540 *Theobroma cacao* (48) as an outgroup.

541 The publicly available C/C<sub>1</sub> gene lists and QTL intervals were  
 542 generated against the v2 maize assembly. To make this comparable to  
 543 the across-grass and NAM parent GENESPACE runs, we also  
 544 accomplished a fast GENESPACE run between v2 and the two v5  
 545 versions used here. The orthologs and synteny mapping between  
 546 these versions are included as text files in the data repository.

547 Statistics presented here were all calculated within R. To compare  
 548 non-normal distributions (e.g. sequence identity), we used the non-

**Table 3 | Raw data sources. A list of the genomes used in analyses here.** Genome version IDs are taken from those posted on the respective data sources and may not reflect the name of the genome in the publication. Where multiple haplotypes are available, only the primary was used for these analyses. All polyploids presented here have only a primary haplotype assembled into chromosomes.

ID	Species	Genome version	Data source	Ploidy*	Reference
garterSnake	<i>Thamnophis elegans</i>	rThaEle1.pri	NCBI	1	(11)
sandLizard	<i>Lacerta agilis</i>	rLacAgi1.pri	NCBI	1	(11)
chicken	<i>Gallus gallus</i>	mat.broiler.GRCg7b	NCBI	1	<a href="https://www.ncbi.nlm.nih.gov/grc">https://www.ncbi.nlm.nih.gov/grc</a>
hummingbird	<i>Calypte anna</i>	bCalAnn1_v1.p	NCBI	1	(11)
budgie	<i>Melopsittacus undulatus</i>	bMelUnd1.mat.Z	NCBI	1	Unpublished VGP
swan	<i>Cygnus olor</i>	bCygOlo1.pri.v2	NCBI	1	(11)
zebraFinch	<i>Taeniopygia guttata</i>	bTaeGut1.4.pri	NCBI	1	(11)
echidna	<i>Tachyglossus aculeatus</i>	mTacAcu1.pri	NCBI	1	(34)
platypus	<i>Ornithorhynchus anatinus</i>	mOrnAna1.pri.v4	NCBI	1	(34)
brushtailPossum	<i>Trichosurus vulpecula</i>	mmTriVul1.pri	NCBI	1	(11)
opossum	<i>Monodelphis domestica</i>	MonDom5	NCBI	1	(35)
tasmanianDevil	<i>Sarcophilus harrisii</i>	mSarHar1.11	NCBI	1	(11)
human	<i>Homo sapiens</i>	GRCh38.p13	NCBI	1	<a href="https://www.ncbi.nlm.nih.gov/grc">https://www.ncbi.nlm.nih.gov/grc</a>
mouse	<i>Mus musculus</i>	GRCm39	NCBI	1	<a href="https://www.ncbi.nlm.nih.gov/grc">https://www.ncbi.nlm.nih.gov/grc</a>
dog	<i>Canis lupus familiaris</i>	Dog10K_Boxer_Tasha	NCBI	1	(36)
sloth	<i>Choloepus didactylus</i>	mChoDid1.pri	NCBI	1	(11)
horseshoeBat	<i>Rhinolophus ferrumequinum</i>	mRhiFer1_v1.p	NCBI	1	(11)
dolphin	<i>Tursiops truncatus</i>	mTurTru1.mat.Y	NCBI	1	Unpublished VGP
Phallii	<i>Panicum hallii</i> var. <i>hallii</i>	HAL2_v2.1	Phytozome	1	(9)
switchgrass	<i>Panicum virgatum</i>	AP13_v5.1	Phytozome	2	(19)
Sviridis	<i>Setaria viridis</i>	v2.1	Phytozome	1	(37)
Sorghum	<i>Sorghum bicolor</i>	BTx623_v3.1	Phytozome	1	(38)
maize	<i>Zea mays</i>	B73_refgen_v5	NCBI	*2	(24)
rice	<i>Oryza sativa</i> cv 'kitaake'	kitaake_v2.1	Phytozome	1	(39)
brachy	<i>Brachypodium distachyon</i>	Bd21_v3.1	Phytozome	1	(40)
wheat	<i>Triticum aestivum</i>	V4 (Chinese Spring)	NCBI	3	(41)
Gbarbadense	<i>Gossypium barbadense</i>	v1.1	Phytozome	2	(12)
Gdarwinii	<i>Gossypium darwinii</i>	v1.1	Phytozome	2	(12)
Gtomentosum	<i>Gossypium tomentosum</i>	v1.1	Phytozome	2	(12)
26 NAM parents	<i>Zea mays</i>	see data on NCBI	NCBI	*1	(24)

\*Ploidy indicates how the genome was treated in the analyses. All values match the ploidy of the primary assembly haplotype except maize, where the refgen\_v5 was treated as diploid (to match both homeologs) in the multi-species run, but as haploid in the NAM founder population to track only meiotic homologs across the population. This parameterization is to match the phylogenetic position of the WGD in the terminal branch of the grass-wide analysis, but ancestral in the 26-NAM analysis.

parametric signed Wilcoxon ranked sum test. To measure sequence divergence, we conducted pairwise peptide alignments via Needleman-Wunsch global alignment, implemented in the Biostings (45) function, pairwiseAlignment. We then used this alignment to calculate the percent peptide sequence identity between the ungapped aligned regions for any two single-copy anchor hits using the Biostings function pid with the type2 method. To determine single outliers from a unimodal distribution, we applied the Grubbs test implemented in the outliers R package (49). Some figures were constructed outside of GENESPACE using base R plotting routines and ggplot2 v3.3.3 (50). Some color palettes were chosen with RColorBrewer (51) and viridis (52).

### 563 GENESPACE pipeline: Running orthofinder within R

564 GENESPACE operates on gff3-formatted annotation files and 565 accompanying peptide fasta files for primary gene models. There are 566 convenience functions for re-formatting the gff and peptide files to 567 simplify the naming scheme and reduce redundant gene models to the 568 primary longest transcript. With these data in hand OrthoFinder (1) is 569 run on the parsed primary peptide files. While the default behavior of 570 GENESPACE is to run OrthoFinder using its default parameters 571 (diamond2 --more-sensitive), GENESPACE also offers a 'fast' method 572 that performs only one-way diamond2 (47) searches, where the 573 genome annotation with more gene models serves as the query and 574 the smaller annotation is the target. The diamond BLAST-like (hereon 575 'BLAST') results are mirrored and each are stored as OrthoFinder- 576 formatted blast8 text files. OrthoFinder is then run to the orthogroup- 577 forming step (-og) on the pre-computed BLAST text files. This

578 method results in significant speed improvements with little loss of 579 fidelity among closely-related haploid genomes (Table 4).

580 There are two methods to infer orthogroups; the original (-og) 581 method clusters genes and builds an undirected cyclic graph from 582 closely related genes bases on BLAST scores (2), while hierarchical 583 phylogenetic orthogroups can disarticulate the clustered orthogroups 584 based on gene trees (7). The latter approach may more effectively 585 exclude paralogs from orthogroups (Supplemental Table 1). Finally, 586 orthofinder infers pairwise orthologs as directed acyclic graphs from 587 one genome to each other (1). The orthologs represent the most strict 588 definition of orthology and are based on gene trees. GENESPACE 589 attempts to merge the benefits of each of these methods by first, only 590 considering -og orthogroups for synteny, which allows users to 591 optionally include paralogs in the scan. If hierarchical orthogroups 592 were used instead, a dramatic decrease in homeologous gene 593 discovery would be expected. To take advantage of the more 594 advanced orthofinder methods, GENESPACE includes non-syntenic 595 gene tree-inferred orthologs into the pan-genome annotation during its 596 final steps (see below).

597 Orthofinder defines orthogroups as the set of genes that are 598 descended from a single gene in the last common ancestor of all the 599 species being considered. As such, the scale of the orthofinder run 600 matters, often significantly. For example, an orthogroup would not be 601 likely to contain homeologs across the two ancient sub-genomes for 602 an orthofinder run that included only two maize genomes — since the 603 coalescence of any two maize genotypes occurred well before the 604 ~12M ya whole genome duplication, few homeologs would both be 605 descended from the same common ancestor when considering only

606 maize genotypes. This is why the within-maize NAM parent run (Fig. 607 2d) excludes homeologs. However, if an outgroup to maize is included 608 in the orthofinder run, both maize homeologs would be likely to show 609 common ancestry to a single gene in the outgroup, thus connecting 610 the maize homeologs into a single orthogroup. This is why both maize 611 homeologous regions are present in the across-grasses synteny graph 612 (Fig. 2a) despite using identical parameters to the maize NAM parent 613 run. Given the potentially significant role of outgroups on the results of 614 the global orthofinder run (Supplemental Table 1), GENESPACE offers 615 an “outgroup” parameters, which specifies which of the genomes 616 should be included in the orthofinder run, but excluded for all 617 downstream analyses.

618

#### 619 GENESPACE pipeline: Build syntenic orthogroup graphs

620 Syntenic regions are extracted from BLAST hit files with graph- 621 and cluster-based approaches using a set of user-defined parameters. 622 While these parameters allow for flexibility, the defaults are sufficient 623 for most high-quality genomes and evolutionary scenarios; for 624 example, we used the same default parameters for 300M years of 625 vertebrate evolution, 65M years and multiple WGDs of grasses, and 626 10k years of Maize divergence. For a full list of parameters, see 627 documentation of the `set_syntenyParams` GENESPACE function, but 628 here, we will discuss the (1) the minimum number of unique hits within 629 a syntenic block ('blkSize', default = 5), (2) the maximum number of 630 gaps within a block alignment ('nGaps', default = 5), and (3) the radius 631 around a syntenic anchor for a hit to be considered syntenic ('synBuff', 632 default = 100).

633 Prior to pairwise synteny searches, ‘collinear arrays’ are defined 634 for each genome as groups of genes separated by no more than 635 synBuff genes on the same chromosome that share an orthogroup. For 636 each collinear array, the single physically most central gene is flagged 637 as the ‘array representative’. Only the array representatives can be 638 syntenic anchors (see below); this culling produces more accurate 639 block coordinates in regions with large tandem arrays (Table 2) and 640 substantial speed improvements in highly repetitive genomes.

641 **Table 4 | Comparison of GENESPACE setting performance.** The 642 mirrored ‘fast’ method significantly speeds up orthofinder runs by calling 643 diamond blastp --fast on each non-redundant pairwise combination of 644 genomes. However, this approach is less sensitive than the default 645 performance and is suggested for only closely-related haploid genomes, as 646 the recall of 2:2:2 OGs is slightly less sensitive than the default specification.

	Default orthofinder	GENESPACE ‘fast’
n. 1:1:1 OGs	22,050	22,444
n. 2:2:2 OGs	13,793	13,511
n. tandem arrays	10,597 (4433)	10,599 (4426)
*Run time (minutes)	59.95	12.45

647 \*Run time is for ortholog/orthogroup inference, not the GENESPACE pipeline 648 as a whole, using the three unsplit cotton genomes, running on 6 2Gb cores.

649 For each pairwise combination of genomes, synteny is inferred in 650 three steps: (1) the potential syntenic anchor hits are extracted as the 651 top n hits for each array representative gene (where n is the expected 652 ploidy of the alternate genome); (2) collinear anchors are defined by 653 MCScanX; (3) hits within a buffer radius of the collinear anchors are 654 extracted by dbscan. For intra-genomic searches within a haploid 655 genome, synteny is simply defined as the region within the synBuff of 656 self hits. Intra-genomic searches within polyploids (or outbred diploids) 657 are more complicated, as self-hits will cause non-self regions to appear 658 highly broken up. To resolve this issue, the self-hit regions are masked 659 and syntenic regions are calculated on the non-self space following the 660 method for inter-genomic synteny. Syntenic orthogroups, which are 661 initially defined as synteny-constrained global orthogroups, can be 662 updated to include re-calculated within-block orthogroups. This step 663 is computationally intensive and yields significantly improved results 664 only when one or more of the genomes are not haploid (Table 1). As 665 such, the default behavior of GENESPACE is to only run within-block 666 OrthoFinder when any of the genomes have diploid or higher ploidy.

667

#### 668 GENESPACE pipeline: Constructing pan-genome annotations

669 Pairwise syntenic orthologs are decoded into a multi-genome pan- 670 annotation, which is represented by a text file containing the expected 671

672 position of all syntenic orthologs across all genomes. This dataset is 673 built in three steps: First, a reference pan-genome annotation is built 674 for all syntenic orthogroups that include a hit in the user-specified 675 reference genome, producing a synteny-aware database that 676 represents each directed subgraph containing a reference genome 677 gene across all genomes. Second, the expected physical position of 678 all genes are interpolated from the syntenic block anchor hits and 679 orthogroups missing from the reference pan-genome annotation are 680 added accordingly, which permits inference of presence-absence 681 variation within a physical position. These interpolated positions are 682 integrated into the pan-genome annotation where each subgraph in 683 the pan-genome is checked as to whether it has a representative 684 anchored in the reference pan-genome. Third, non-syntenic orthologs 685 are extracted from the raw orthofinder run and added to the pan- 686 genome annotation. The reference pan-genome contains all syntenic 687 orthogroup hits connected by a directed acyclic graph to a reference 688 gene. However, there are many cases where the reference gene in this 689 graph is not the only mapping to the reference. For example, polyploids 690 should have multiple positions. As such, we need to cluster the 691 reference positions of all genes in all subgraphs to ensure that all 692 syntenic positions and PAV are captured accurately.

693

## 694 FOOTNOTES

695

### 696 Acknowledgements

697 The GENESPACE pipeline has been improved by advice and 698 testing by A. Healey, N. Walden, V. Markham, R. Walstead, S. Carey, 699 L. Smith, J. Vogel, J. Willis, J. Jenkins, T. Juenger and many others. 700 Thanks to J. Schnable, J. Leebens-Mack, J.G. Monroe, C.H. Li, R. 701 Tarvin, and M. Hufford for help refining the datasets and analyses 702 presented in this manuscript. Thank you to Erich D. Jarvis and the 703 Vertebrate Genome Project members for advice and pre-publication 704 access to several genomes (budgerigar and dolphin). The work 705 conducted by the US Department of Energy Joint Genome Institute is 706 supported by the Office of Science of the US Department of Energy 707 under Contract No DE-AC02-05CH1123. Visualization was inspired in 708 part by MCScanX and pairwise ‘river’ plots generated by other 709 software. The use of syntenic orthogroups was originally inspired by 710 work developed by CoGe. MAW’s work on this was supported by the 711 National Institute of General Medical Sciences (NIGMS) of the National 712 Institutes of Health (NIH) grant R35GM124827. JTL would like to thank 713 Ashley Lovell, our friends and family for their support, which allowed 714 him to work on this project during the difficult past two years.

715

### 716 Data availability

717 Raw data was sourced entirely from NCBI and Phytozome. 718 Processed data, intermediate files, scripts, plots and source 719 data are all available in the data repository: 720 [https://github.com/jtlovell/GENESPACE\\_data](https://github.com/jtlovell/GENESPACE_data). All source code 721 and documentation for the GENESPACE R package can be 722 found at <https://github.com/jtlovell/GENESPACE>. An interactive 723 viewer for the plant genomes can be found on phytozome at 724 <https://phytozome-next.jgi.doe.gov/tools/dotplot/synteny.html>.

725

### 726 Description of supplemental data

727 **Supplemental Data 1.** Pan-genome annotation of the 728 vertebrates using the human genome as the reference coordinate 729 system. For each row (pan-genome entry), there is position 730 information, projected against the gene order coordinate system of 731 the human genome; pgChr and pgOrd are the human chromosome 732 and gene rank order position of that entry. There is also a pgID 733 column, which splits entries that happen to be at the same position 734 but lack a reference gene. The remaining columns are the 17 735 vertebrate genome IDs. In each column, syntenic orthogroup (un- 736 flagged), non-syntenic orthologs (flagged \*) and tandem array 737 members (flagged +) are ‘|’ separated.

738

739 **Supplemental Data 2.** Pan-genome annotation of the 740 vertebrates using the chicken genome gene rank order as the 741 reference coordinate system. Columns follow supplemental data 1.

732 **Supplemental Data 3.** Physical coordinates of syntenic block  
733 breakpoints among all pairwise combinations of the 17 vertebrate  
734 genomes. Pairwise combinations are distinguished by the genome  
735 IDs presented in the first two columns. The following six columns  
736 (chr1, chr2, start1, start2, end1, end2) are separated where columns  
737 ending in “1” belong to the coordinate system of the genome ID in  
738 the first “genome1” column, while columns ending in “2” belong to  
739 the coordinate system of the genome ID in the second “genome2”  
740 column. Start and end coordinates are in base pairs. Orientation,  
741 column “orient” is flagged as “+” for collinear, “-” for inverted. The  
742 last column, “nhits” is the number of syntenic anchor hits within that  
743 block.

744 **Supplemental Data 4.** Physical coordinates of syntenic block  
745 breakpoints among all pairwise combinations of the 8 grass  
746 genomes. Columns follow supplemental data 3.

747 **Supplemental Data 5.** Pan-genome annotation of the grasses  
748 using the maize B73 genome gene rank order as the reference  
749 coordinate system. Columns follow supplemental data 1.

750 **Supplemental Data 6.** Physical coordinates of syntenic block  
751 breakpoints among all pairwise combinations of the 26 NAM parents.  
752 Columns follow supplemental data 3.

753 **Supplemental Data 7.** Pan-genome annotation of the 26 NAM  
754 parents using the maize B73 genome gene rank order as the  
755 reference coordinate system. Columns follow supplemental data 1.

756 **Supplemental Data 8.** Pan-genome entries of the 26 maize NAM  
757 founders for each of the three QTL regions in Li et al. 2016. Columns  
758 follow supplemental data 1, with the additional first column “qtl”,  
759 which holds the QTL id, coded as [phenotype] [[private focal  
760 genome]: [chromosome], [start Mbp]-[end Mbp].

761 **Supplemental Data 9.** Pan-genome annotation of the grasses,  
762 explicitly including the *Rho*-duplicated homologs into the graph, and  
763 using the *S. viridis* genome as the reference coordinate system.  
764 Columns follow supplemental data 1.

765 **Supplemental Data 10.** Hits between *P. hallii* and *S. viridis*  
766 genes that are members of the same within-block orthogroups and  
767 are syntenic anchors. The first 12 columns (id1, id2, genome1,  
768 genome2, chr1, chr2, start1, end1, ord1, start2, end2, ord2) are  
769 separated where columns ending in “1” belong to the coordinate  
770 system of the genome ID in the first “genome1” column, while  
771 columns ending in “2” belong to the coordinate system of the  
772 genome ID in the second “genome2” column. Start and end are bp  
773 positions, ord is the gene rank order. The two measures of percent  
774 protein identity are given in pid1 and pid2 columns. The block type,  
775 categorized as orthologous (“orth”), over-retained *Rho* paralog  
776 (“overr”), regular *Rho* paralog (“rho”) and ambiguous (“ambig”) are  
777 given in the column blockType.

778

## REFERENCES

780 1. D. M. Emms, S. Kelly, OrthoFinder: phylogenetic orthology  
781 inference for comparative genomics. *Genome Biol.* **20**, 238  
782 (2019).

783 2. D. M. Emms, S. Kelly, OrthoFinder: solving fundamental biases  
784 in whole genome comparisons dramatically improves  
785 orthogroup inference accuracy. *Genome Biol.* **16**, 157 (2015).

786 3. A. Haug-Baltzell, S. A. Stephens, S. Davey, C. E. Scheidegger,  
787 E. Lyons, SynMap2 and SynMap3D: web-based whole-genome  
788 synteny browsers. *Bioinformatics*. **33**, 2197–2198 (2017).

789 4. Y. Wang, H. Tang, J. D. Debarry, X. Tan, J. Li, X. Wang, T.-H.  
790 Lee, H. Jin, B. Marler, H. Guo, J. C. Kissinger, A. H. Paterson,  
791 MCScanX: a toolkit for detection and evolutionary analysis of  
792 gene synteny and collinearity. *Nucleic Acids Res.* **40**, e49 (2012).

793 5. G. Drillon, R. Champeimont, F. Oteri, G. Fischer, A. Carbone,  
794 Phylogenetic Reconstruction Based on Synteny Block and Gene  
795 Adjacencies. *Mol. Biol. Evol.* **37**, 2747–2762 (2020).

796 6. O. Simakov, F. Marlétaz, J.-X. Yue, B. O’Connell, J. Jenkins, A.  
797 Brandt, R. Calef, C.-H. Tung, T.-K. Huang, J. Schmutz, N.  
798 Satoh, J.-K. Yu, N. H. Putnam, R. E. Green, D. S. Rokhsar,  
799 7. Y. Jiao, J. Li, H. Tang, A. H. Paterson, Integrated syntenic and  
800 phylogenomic analyses reveal an ancient genome duplication in  
801 monocots. *Plant Cell*. **26**, 2792–2802 (2014).

802 8. T. Zhao, M. Eric Schranz, Network-based microsynteny analysis  
803 identifies major differences and genomic outliers in mammalian  
804 and angiosperm genomes. *Proc. Natl. Acad. Sci. U. S. A.* **116**,  
805 2165–2174 (2019).

806 9. J. T. Lovell, J. Jenkins, D. B. Lowry, S. Mamidi, A. Sreedasyam,  
807 X. Weng, K. Barry, J. Bonnette, B. Campitelli, C. Daum, S. P.  
808 Gordon, B. A. Gould, A. Khasanova, A. Lipzen, A. MacQueen, J.  
809 D. Palacio-Mejia, C. Plott, E. V. Shakirov, S. Shu, Y. Yoshinaga,  
810 M. Zane, D. Kudrna, J. D. Talag, D. Rokhsar, J. Grimwood, J.  
811 Schmutz, T. E. Juenger, The genomic landscape of molecular  
812 responses to natural drought stress in *Panicum hallii*. *Nat.*  
813 *Commun.* **9**, 5213 (2018).

814 10. J. T. Lovell, N. B. Bentley, G. Bhattarai, J. W. Jenkins, A.  
815 Sreedasyam, Y. Alarcon, C. Bock, L. B. Boston, J. Carlson, K.  
816 Cervantes, K. Clermont, S. Duke, N. Krom, K. Kubenka, S.  
817 Mamidi, C. P. Mattison, M. J. Monteros, C. Pisani, C. Plott, S.  
818 Rajasekar, H. S. Rhein, C. Rohla, M. Song, R. S. Hilaire, S. Shu,  
819 L. Wells, J. Webber, R. J. Heerema, P. E. Klein, P. Conner, X.  
820 Wang, L. J. Grauke, J. Grimwood, J. Schmutz, J. J. Randall,  
821 Four chromosome scale genomes and a pan-genome  
822 annotation to accelerate pecan tree breeding. *Nat. Commun.* **12**,  
823 4125 (2021).

824 11. A. Rhie, S. A. McCarthy, O. Fedrigo, J. Damas, G. Formenti, S.  
825 Koren, M. Uliano-Silva, W. Chow, A. Fungtammasan, J. Kim, C.  
826 Lee, B. J. Ko, M. Chaisson, G. L. Gedman, L. J. Cantin, F.  
827 Thibaud-Nissen, L. Haggerty, I. Bista, M. Smith, B. Haase, J.  
828 Mountcastle, S. Winkler, S. Paez, J. Howard, S. C. Vernes, T. M.  
829 Lama, F. Grutzner, W. C. Warren, C. N. Balakrishnan, D. Burt, J.  
830 M. George, M. T. Biegler, D. Iorns, A. Digby, D. Eason, B.  
831 Robertson, T. Edwards, M. Wilkinson, G. Turner, A. Meyer, A. F.  
832 Kautt, P. Franchini, H. W. Detrich 3rd, H. Svardal, M. Wagner, G.  
833 J. P. Naylor, M. Pippel, M. Malinsky, M. Mooney, M. Simbirskey,  
834 B. T. Hannigan, T. Pesout, M. Houck, A. Misuraca, S. B. Kingan,  
835 R. Hall, Z. Kronenberg, I. Sović, C. Dunn, Z. Ning, A. Hastie, J.  
836 Lee, S. Selvaraj, R. E. Green, N. H. Putnam, I. Gut, J. Ghurye, E.  
837 Garrison, Y. Sims, J. Collins, S. Pelan, J. Torrance, A. Tracey, J.  
838 Wood, R. E. Dagnew, D. Guan, S. E. London, D. F. Clayton, C.  
839 V. Mello, S. R. Friedrich, P. V. Lovell, E. Osipova, F. O. Al-Ajli, S.  
840 Secomandi, H. Kim, C. Theofanopoulou, M. Hiller, Y. Zhou, R. S.  
841 Harris, K. D. Makova, P. Medvedev, J. Hoffman, P. Masterson,  
842 K. Clark, F. Martin, K. Howe, P. Flieck, B. P. Walenz, W. Kwak,  
843 H. Clawson, M. Diekhans, L. Nassar, B. Paten, R. H. S. Kraus, A.  
844 J. Crawford, M. T. P. Gilbert, G. Zhang, B. Venkatesh, R. W.  
845 Murphy, K.-P. Koepfli, B. Shapiro, W. E. Johnson, F. Di Palma,  
846 T. Marques-Bonet, E. C. Teeling, T. Warnow, J. M. Graves, O. A.  
847 Ryder, D. Haussler, S. J. O’Brien, J. Korlach, H. A. Lewin, K.  
848 Howe, E. W. Myers, R. Durbin, A. M. Phillippy, E. D. Jarvis,  
849 Towards complete and error-free genome assemblies of all  
850 vertebrate species. *Nature*. **592**, 737–746 (2021).

851 12. Z. J. Chen, A. Sreedasyam, A. Ando, Q. Song, L. M. De  
852 Santiago, A. M. Hulse-Kemp, M. Ding, W. Ye, R. C. Kirkbride, J.  
853 Jenkins, C. Plott, J. Lovell, Y.-M. Lin, R. Vaughn, B. Liu, S.  
854 Simpson, B. E. Scheffler, L. Wen, C. A. Saski, C. E. Grover, G.  
855 Hu, J. L. Conover, J. W. Carlson, S. Shu, L. B. Boston, M.  
856 Williams, D. G. Peterson, K. McGee, D. C. Jones, J. F. Wendel,  
857 D. M. Stelly, J. Grimwood, J. Schmutz, Genomic diversifications  
858 of five *Gossypium* allopolyploid species and their impact on  
859 cotton improvement. *Nat. Genet.* **52**, 525–533 (2020).

860 13. W. J. Murphy, S. Sun, Z. Q. Chen, J. Pecon-Slattery, S. J.  
861 O’Brien, Extensive conservation of sex chromosome  
862 organization between cat and human revealed by parallel  
863 radiation hybrid mapping. *Genome Res.* **9**, 1223–1230 (1999).

864 14. Q. Zhou, J. Zhang, D. Bachtrog, N. An, Q. Huang, E. D. Jarvis,  
865 M. T. P. Gilbert, G. Zhang, Complex evolutionary trajectories of  
866 sex chromosomes across bird taxa. *Science*. **346**, 1246338

869 (2014).

870 15. L. Kratochvíl, T. Gamble, M. Rovatsos, Sex chromosome  
871 evolution among amniotes: is the origin of sex chromosomes  
872 non-random? *Philos. Trans. R. Soc. Lond. B Biol. Sci.* **376**,  
873 20200108 (2021).

874 16. M. T. Ross, D. V. Grafham, A. J. Coffey, S. Scherer, K. McLay,  
875 D. Muzny, M. Platzer, G. R. Howell, C. Burrows, C. P. Bird, A.  
876 Frankish, F. L. Lovell, K. L. Howe, J. L. Ashurst, R. S. Fulton, R.  
877 Sudbrak, G. Wen, M. C. Jones, M. E. Hurles, T. D. Andrews, C.  
878 E. Scott, S. Searle, J. Ramser, A. Whittaker, R. Deadman, N. P.  
879 Carter, S. E. Hunt, R. Chen, A. Cree, P. Gunaratne, P. Havlak, A.  
880 Hodgson, M. L. Metzker, S. Richards, G. Scott, D. Steffen, E.  
881 Sodergren, D. A. Wheeler, K. C. Worley, R. Ainscough, K. D.  
882 Ambrose, M. A. Ansari-Lari, S. Aradhya, R. I. S. Ashwell, A. K.  
883 Babbage, C. L. Baggaley, A. Ballabio, R. Banerjee, G. E. Barker,  
884 K. F. Barlow, I. P. Barrett, K. N. Bates, D. M. Beare, H. Beasley,  
885 O. Beasley, A. Beck, G. Bethel, K. Blechschmidt, N. Brady, S.  
886 Bray-Allen, A. M. Bridgeman, A. J. Brown, M. J. Brown, D.  
887 Bonnici, E. A. Bruford, C. Buhay, P. Burch, D. Burford, J.  
888 Burgess, W. Burrill, J. Burton, J. M. Bye, C. Carder, L. Carrel, J.  
889 Chako, J. C. Chapman, D. Chavez, E. Chen, G. Chen, Y. Chen,  
890 Z. Chen, C. Chinault, A. Ciccodicola, S. Y. Clark, G. Clarke, C.  
891 M. Cleo, S. Clegg, K. Clerc-Blankenburg, K. Clifford, V. Cobley,  
892 C. G. Cole, J. S. Conquer, N. Corby, R. E. Connor, R. David, J.  
893 Davies, C. Davis, J. Davis, O. Delgado, D. Deshazo, P. Dhami, Y.  
894 Ding, H. Dinh, S. Dodsworth, H. Draper, S. Dugan-Rocha, A.  
895 Dunham, M. Dunn, K. J. Durbin, I. Dutta, T. Eades, M. Ellwood,  
896 A. Emery-Cohen, H. Errington, K. L. Evans, L. Faulkner, F.  
897 Francis, J. Frankland, A. E. Fraser, P. Galgoczy, J. Gilbert, R.  
898 Gill, G. Glöckner, S. G. Gregory, S. Gribble, C. Griffiths, R.  
899 Grocock, Y. Gu, R. Gwilliam, C. Hamilton, E. A. Hart, A. Hawes,  
900 P. D. Heath, K. Heitmann, S. Hennig, J. Hernandez, B.  
901 Hinzmann, S. Ho, M. Hoffs, P. J. Howden, E. J. Huckle, J.  
902 Hume, P. J. Hunt, A. R. Hunt, J. Isherwood, L. Jacob, D.  
903 Johnson, S. Jones, P. J. de Jong, S. S. Joseph, S. Keenan, S.  
904 Kelly, J. K. Kershaw, Z. Khan, P. Kioschis, S. Klages, A. J.  
905 Knights, A. Kosiura, C. Kovar-Smith, G. K. Laird, C. Langford, S.  
906 Lawlor, M. Leversha, L. Lewis, W. Liu, C. Lloyd, D. M. Lloyd, H.  
907 Loulseged, J. E. Loveland, J. D. Lovell, R. Lozano, J. Lu, R.  
908 Lyne, J. Ma, M. Maheshwari, L. H. Matthews, J. McDowell, S.  
909 McLaren, A. McMurray, P. Meidl, T. Meitinger, S. Milne, G.  
910 Miner, S. L. Mistry, M. Morgan, S. Morris, I. Müller, J. C. Mullikin,  
911 N. Nguyen, G. Nordsiek, G. Nyakatara, C. N. O'Dell, G.  
912 Okwuonu, S. Palmer, R. Pandian, D. Parker, J. Parrish, S.  
913 Pasternak, D. Patel, A. V. Pearce, D. M. Pearson, S. E. Pelan, L.  
914 Perez, K. M. Porter, Y. Ramsey, K. Reichwald, S. Rhodes, K. A.  
915 Ridler, D. Schlessinger, M. G. Schueler, H. K. Sehra, C. Shaw-  
916 Smith, H. Shen, E. M. Sheridan, R. Showkenne, C. D. Skuce, M.  
917 L. Smith, E. C. Sotheran, H. E. Steingrubler, C. A. Steward, R.  
918 Storey, R. M. Swann, D. Swarbreck, P. E. Tabor, S. Taudien, T.  
919 Taylor, B. Teague, K. Thomas, A. Thorpe, K. Timms, A. Tracey,  
920 S. Trevanion, A. C. Tromans, M. d'Urso, D. Verduzco, D.  
921 Villasana, L. Waldron, M. Wall, Q. Wang, J. Warren, G. L. Warry,  
922 X. Wei, A. West, S. L. Whitehead, M. N. Whiteley, J. E.  
923 Wilkinson, D. L. Willey, G. Williams, L. Williams, A. Williamson,  
924 H. Williamson, L. Wilming, R. L. Woodmansey, P. W. Wray, J.  
925 Yen, J. Zhang, J. Zhou, H. Zoghbi, S. Zorilla, D. Buck, R.  
926 Reinhardt, A. Poustka, A. Rosenthal, H. Lehrach, A. Meindl, P. J.  
927 Minx, L. W. Hillier, H. F. Willard, R. K. Wilson, R. H. Waterston,  
928 C. M. Rice, M. Vaudin, A. Coulson, D. L. Nelson, G. Weinstock,  
929 J. E. Sulston, R. Durbin, T. Hubbard, R. A. Gibbs, S. Beck, J.  
930 Rogers, D. R. Bentley, The DNA sequence of the human X  
931 chromosome. *Nature*. **434**, 325–337 (2005).

932 17. W. Rens, P. C. M. O'Brien, F. Grützner, O. Clarke, D.  
933 Graphodatskaya, E. Tsend-Ayush, V. A. Trifonov, H. Skelton, M.  
934 C. Wallis, S. Johnston, F. Veyrunes, J. A. M. Graves, M. A.  
935 Ferguson-Smith, The multiple sex chromosomes of platypus  
936 and echidna are not completely identical and several share  
937 homology with the avian Z. *Genome Biol.* **8**, R243 (2007).

938 18. B. S. Gaut, J. F. Doebley, DNA sequence evidence for the  
939 segmental allotetraploid origin of maize. *Proc. Natl. Acad. Sci.*  
940 U. S. A.

941 19. J. T. Lovell, A. H. MacQueen, S. Mamidi, J. Bonnette, J. Jenkins,  
942 J. D. Napier, A. Sreedasyam, A. Healey, A. Session, S. Shu, K.  
943 Barry, S. Bonos, L. Boston, C. Daum, S. Deshpande, A. Ewing,  
944 P. P. Grabowski, T. Haque, M. Harrison, J. Jiang, D. Kudrna, A.  
945 Lipzen, T. H. Pendergast 4th, C. Plott, P. Qi, C. A. Sasaki, E. V.  
946 Shakirov, D. Sims, M. Sharma, R. Sharma, A. Stewart, V. R.  
947 Singan, Y. Tang, S. Thibivillier, J. Webber, X. Weng, M. Williams,  
948 G. A. Wu, Y. Yoshinaga, M. Zane, L. Zhang, J. Zhang, K. D.  
949 Behrman, A. R. Boe, P. A. Fay, F. B. Fritschi, J. D. Jastrow, J.  
950 Lloyd-Reilly, J. M. Martínez-Reyna, R. Matamala, R. B.  
951 Mitchell, F. M. Rouquette Jr, P. Ronald, M. Saha, C. M. Tobias,  
952 M. Urdvardi, R. A. Wing, Y. Wu, L. E. Bartley, M. Casler, K. M.  
953 Devos, D. B. Lowry, D. S. Rokhsar, J. Grimwood, T. E. Juenger,  
954 J. Schmutz, Genomic mechanisms of climate adaptation in  
955 polyploid bioenergy switchgrass. *Nature*. **590**, 438–444 (2021).

956 20. M. Haas, M. Schreiber, M. Mascher, Domestication and crop  
957 evolution of wheat and barley: Genes, genomics, and future  
958 directions. *J. Integr. Plant Biol.* **61**, 204–225 (2019).

959 21. D. M. Goodstein, S. Shu, R. Howson, R. Neupane, R. D. Hayes,  
960 J. Fazo, T. Mitros, W. Dirks, U. Hellsten, N. Putnam, D. S.  
961 Rokhsar, Phytozome: a comparative platform for green plant  
962 genomics. *Nucleic Acids Res.* **40**, D1178–86 (2012).

963 22. Z. Ding, S. Weissmann, M. Wang, B. Du, L. Huang, L. Wang, X.  
964 Tu, S. Zhong, C. Myers, T. P. Brutnell, Q. Sun, P. Li,  
965 Identification of Photosynthesis-Associated C4 Candidate  
966 Genes through Comparative Leaf Gradient Transcriptome in  
967 Multiple Lineages of C3 and C4 Species. *PLoS One*. **10**,  
968 e0140629 (2015).

969 23. C. Li, B. Sun, Y. Li, C. Liu, X. Wu, D. Zhang, Y. Shi, Y. Song, E.  
970 S. Buckler, Z. Zhang, T. Wang, Y. Li, Numerous genetic loci  
971 identified for drought tolerance in the maize nested association  
972 mapping populations. *BMC Genomics*. **17**, 894 (2016).

973 24. M. B. Hufford, A. S. Seetharam, M. R. Woodhouse, K. M.  
974 Chougule, S. Ou, J. Liu, W. A. Ricci, T. Guo, A. Olson, Y. Qiu, R.  
975 Della Coletta, S. Tittes, A. I. Hudson, A. P. Marand, S. Wei, Z.  
976 Lu, B. Wang, M. K. Tello-Ruiz, R. D. Piri, N. Wang, D. W. Kim, Y.  
977 Zeng, C. H. O'Connor, X. Li, A. M. Gilbert, E. Baggs, K. V.  
978 Krasileva, J. L. Portwood 2nd, E. K. S. Cannon, C. M. Andorf, N.  
979 Manchanda, S. J. Snodgrass, D. E. Hufnagel, Q. Jiang, S.  
980 Pedersen, M. L. Syring, D. A. Kudrna, V. Llaca, K. Fengler, R. J.  
981 Schmitz, J. Ross-Ibarra, J. Yu, J. I. Gent, C. N. Hirsch, D. Ware,  
982 R. K. Dawe, De novo assembly, annotation, and comparative  
983 analysis of 26 diverse maize genomes. *Science*. **373**, 655–662  
984 (2021).

985 25. M. S. Barker, N. Arrigo, A. E. Baniaga, Z. Li, D. A. Levin, On the  
986 relative abundance of autopolyploids and allopolyploids. *New  
987 Phytol.* **210**, 391–398 (2016).

988 26. G. Ledyard Stebbins, *Variation and Evolution in Plants*  
989 (Columbia University Press, 1950).

990 27. One Thousand Plant Transcriptomes Initiative, One thousand  
991 plant transcriptomes and the phylogenomics of green plants.  
992 *Nature*. **574**, 679–685 (2019).

993 28. H. J. Muller, Why Polyploidy is Rarer in Animals Than in Plants.  
994 *Am. Nat.* **59**, 346–353 (1925).

995 29. J. C. Preston, E. A. Kellogg, Reconstructing the evolutionary  
996 history of paralogous APETALA1/FRUITFULL-like genes in  
997 grasses (Poaceae). *Genetics*. **174**, 421–437 (2006).

998 30. J. C. Preston, A. Christensen, S. T. Malcomber, E. A. Kellogg,  
999 MADS-box gene expression and implications for developmental  
1000 origins of the grass spikelet. *Am. J. Bot.* **96**, 1419–1429 (2009).

1001 31. Y. Wu, Z. Zhu, L. Ma, M. Chen, The preferential retention of  
1002 starch synthesis genes reveals the impact of whole-genome  
1003 duplication on grass evolution. *Mol. Biol. Evol.* **25**, 1003–1006  
1004 (2008).

1005 32. P.-F. Ma, Y.-L. Liu, G.-H. Jin, J.-X. Liu, H. Wu, J. He, Z.-H. Guo,  
1006 D.-Z. Li, The *Pharus latifolius* genome bridges the gap of early  
1007 grass evolution. *Plant Cell*. **33**, 846–864 (2021).

1006 33. X. Wang, H. Tang, A. H. Paterson, Seventy Million Years of  
1009 Concerted Evolution of a Homoeologous Chromosome Pair, in  
1010 Parallel, in Major Poaceae Lineages. *Plant Cell.* **23**, 27–37  
1011 (2011).

1012 34. Y. Zhou, L. Shearwin-Whyatt, J. Li, Z. Song, T. Hayakawa, D.  
1013 Stevens, J. C. Fenelon, E. Peel, Y. Cheng, F. Pajpach, N.  
1014 Bradley, H. Suzuki, M. Nikaido, J. Damas, T. Daish, T. Perry, Z.  
1015 Zhu, Y. Geng, A. Rhie, Y. Sims, J. Wood, B. Haase, J.  
1016 Mountcastle, O. Fedrigo, Q. Li, H. Yang, J. Wang, S. D.  
1017 Johnston, A. M. Phillipi, K. Howe, E. D. Jarvis, O. A. Ryder, H.  
1018 Kaessmann, P. Donnelly, J. Korlach, H. A. Lewin, J. Graves, K.  
1019 Belov, M. B. Renfree, F. Grützner, Q. Zhou, G. Zhang, Platypus  
1020 and echidna genomes reveal mammalian biology and evolution.  
1021 *Nature.* **592**, 756–762 (2021).

1022 35. T. S. Mikkelsen, M. J. Wakefield, B. Aken, C. T. Amemiya, J. L.  
1023 Chang, S. Duke, M. Garber, A. J. Gentles, L. Goodstadt, A.  
1024 Heger, J. Jurka, M. Kamal, E. Mauceli, S. M. J. Searle, T.  
1025 Sharpe, M. L. Baker, M. A. Batzer, P. V. Benos, K. Belov, M.  
1026 Clamp, A. Cook, J. Cuff, R. Das, L. Davidow, J. E. Deakin, M. J.  
1027 Fazzari, J. L. Glass, M. Grabherr, J. M. Greatly, W. Gu, T. A.  
1028 Hore, G. A. Huttley, M. Kleber, R. L. Jirtle, E. Koina, J. T. Lee, S.  
1029 Mahony, M. A. Marra, R. D. Miller, R. D. Nicholls, M. Oda, A. T.  
1030 Papenfuss, Z. E. Parra, D. D. Pollock, D. A. Ray, J. E. Schein, T.  
1031 P. Speed, K. Thompson, J. L. VandeBerg, C. M. Wade, J. A.  
1032 Walker, P. D. Waters, C. Webber, J. R. Weidman, X. Xie, M. C.  
1033 Zody, Broad Institute Genome Sequencing Platform, Broad  
1034 Institute Whole Genome Assembly Team, J. A. M. Graves, C. P.  
1035 Ponting, M. Breen, P. B. Samollow, E. S. Lander, K. Lindblad-  
1036 Toh, Genome of the marsupial *Monodelphis domestica* reveals  
1037 innovation in non-coding sequences. *Nature.* **447**, 167–177  
1038 (2007).

1039 36. V. Jagannathan, C. Hitte, J. M. Kidd, P. Masterson, T. D.  
1040 Murphy, S. Emery, B. Davis, R. M. Buckley, Y.-H. Liu, X.-Q.  
1041 Zhang, T. Leeb, Y.-P. Zhang, E. A. Ostrander, G.-D. Wang,  
1042 Dog10K\_Boxer\_Tasha\_1.0: A Long-Read Assembly of the Dog  
1043 Reference Genome. *Genes.* **12** (2021), doi:10.3390/genes12060847.

1045 37. S. Mamidi, A. Healey, P. Huang, J. Grimwood, J. Jenkins, K.  
1046 Barry, A. Sreedasyam, S. Shu, J. T. Lovell, M. Feldman, J. Wu,  
1047 Y. Yu, C. Chen, J. Johnson, H. Sakakibara, T. Kiba, T. Sakurai,  
1048 R. Tavares, D. A. Nusinow, I. Baxter, J. Schmutz, T. P. Brutnell,  
1049 E. A. Kellogg, A genome resource for green millet *Setaria viridis*  
1050 enables discovery of agronomically valuable loci. *Nat.*  
1051 *Biotechnol.* **38**, 1203–1210 (2020).

1052 38. A. H. Paterson, J. E. Bowers, R. Bruggmann, I. Dubchak, J.  
1053 Grimwood, H. Gundlach, G. Haberer, U. Hellsten, T. Mitros, A.  
1054 Poliakov, J. Schmutz, M. Spannagl, H. Tang, X. Wang, T.  
1055 Wicker, A. K. Bharti, J. Chapman, F. A. Feltus, U. Gowik, I. V.  
1056 Grigoriev, E. Lyons, C. A. Maher, M. Martis, A. Narechania, R. P.  
1057 Otillar, B. W. Penning, A. A. Salamov, Y. Wang, L. Zhang, N. C.  
1058 Carpita, M. Freeling, A. R. Gingle, C. T. Hash, B. Keller, P. Klein,  
1059 S. Kresovich, M. C. McCann, R. Ming, D. G. Peterson,  
1060 Mehboob-ur-Rahman, D. Ware, P. Westhoff, K. F. X. Mayer, J.  
1061 Messing, D. S. Rokhsar, The *Sorghum bicolor* genome and the  
1062 diversification of grasses. *Nature.* **457**, 551–556 (2009).

1063 39. R. Jain, J. Jenkins, S. Shu, M. Chern, J. A. Martin, D. Copetti, P.  
1064 Q. Duong, N. T. Pham, D. A. Kudrna, J. Talag, W. S. Schackwitz,  
1065 A. M. Lipzen, D. Dilworth, D. Bauer, J. Grimwood, C. R. Nelson,  
1066 F. Xing, W. Xie, K. W. Barry, R. A. Wing, J. Schmutz, G. Li, P. C.  
1067 Ronald, Genome sequence of the model rice variety *KitaakeX*.  
1068 *BMC Genomics.* **20**, 905 (2019).

1069 40. International Brachypodium Initiative, Genome sequencing and  
1070 analysis of the model grass *Brachypodium distachyon*. *Nature.*  
1071 **463**, 763–768 (2010).

1072 41. T. Zhu, L. Wang, H. Rimbert, J. C. Rodriguez, K. R. Deal, R. De  
1073 Oliveira, F. Choulet, G. Keeble-Gagnère, J. Tibbets, J. Rogers, K.  
1074 Eversole, R. Appels, Y. Q. Gu, M. Mascher, J. Dvorak, M.-C.  
1075 Luo, Optical maps refine the bread wheat *Triticum aestivum* cv.  
1076 Chinese Spring genome assembly. *Plant J.* **107**, 303–314 (2021).

1077 42. M. Dowle, A. Srinivasan, *data.table: Extension of 'data.frame'*  
1078 (2021), (available at [https://CRAN.R-  
1079 project.org/package=data.table](https://CRAN.R-project.org/package=data.table)).

1080 43. M. Hahsler, M. Piekenbrock, D. Doran, *dbSCAN: Fast Density-  
1081 Based Clustering with R.* *J. Stat. Softw.* **91** (2019),  
1082 doi:10.18637/jss.v091.i01.

1083 44. G. Csardi, T. Nepusz, Others, The *igraph* software package for  
1084 complex network research. *InterJournal, complex systems.*  
1085 **1695**, 1–9 (2006).

1086 45. H. Pagès, P. Abyoun, R. Gentleman, S. DebRoy, *Biostings:*  
1087 Efficient manipulation of biological strings (2020), (available at  
1088 <https://bioconductor.org/packages/Biostings>).

1089 46. M. Lawrence, R. Gentleman, V. Carey, *rtracklayer: an R package*  
1090 for interfacing with genome browsers. *Bioinformatics.* **25**, 1841–  
1091 1842 (2009).

1092 47. B. Buchfink, K. Reuter, H.-G. Drost, Sensitive protein alignments  
1093 at tree-of-life scale using DIAMOND. *Nat. Methods.* **18**, 366–368  
1094 (2021).

1095 48. J. C. Motamayor, K. Mockaitis, J. Schmutz, N. Haiminen, D.  
1096 Livingstone 3rd, O. Cornejo, S. D. Findley, P. Zheng, F. Utro, S.  
1097 Royaert, C. Saski, J. Jenkins, R. Podicheti, M. Zhao, B. E.  
1098 Scheffler, J. C. Stack, F. A. Feltus, G. M. Mustiga, F. Amores, W.  
1099 Phillips, J. P. Marelli, G. D. May, H. Shapiro, J. Ma, C. D.  
1100 Bustamante, R. J. Schnell, D. Main, D. Gilbert, L. Parida, D. N.  
1101 Kuhn, The genome sequence of the most widely cultivated  
1102 cacao type and its use to identify candidate genes regulating  
1103 pod color. *Genome Biol.* **14**, r53 (2013).

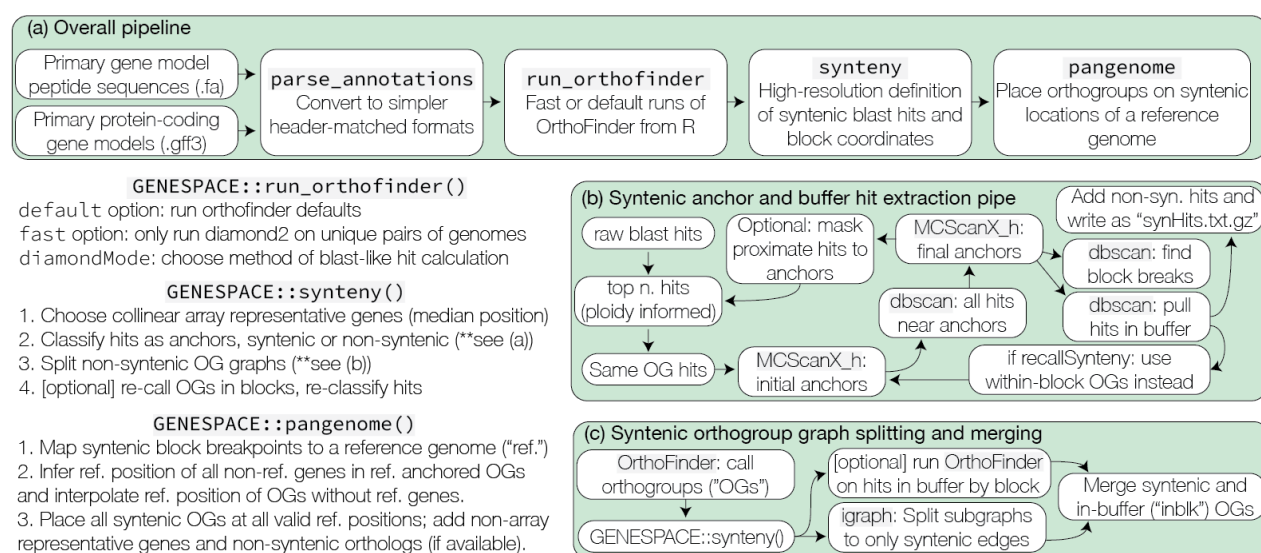
1104 49. L. Komsta, *outliers: Tests for outliers* (2011), (available at  
1105 <https://CRAN.R-project.org/package=outliers>).

1106 50. H. Wickham, *ggplot2: Elegant Graphics for Data Analysis* (2016),  
1107 (available at <https://ggplot2.tidyverse.org>).

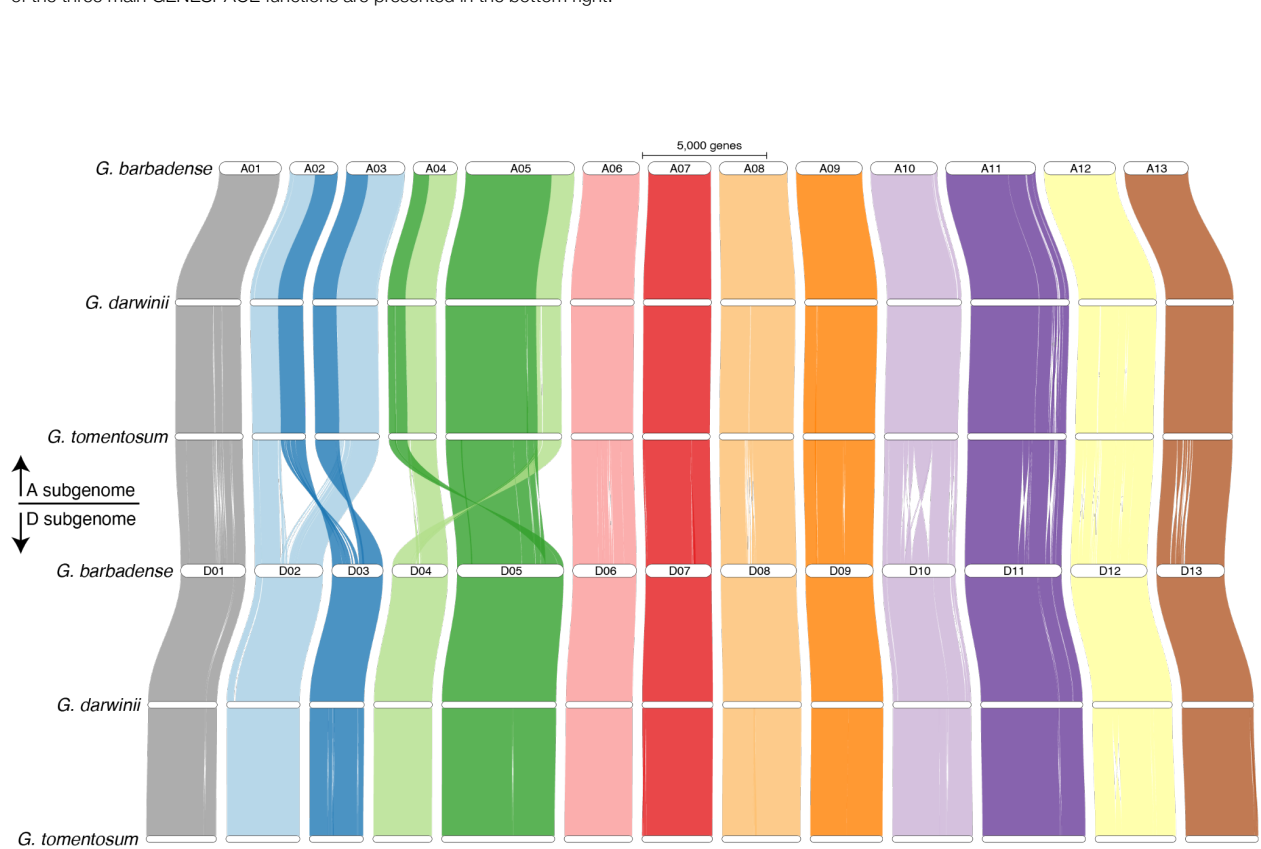
1108 51. E. Neuwirth, *RColorBrewer: ColorBrewer palettes [Software]*  
1109 (2014), (available at [https://CRAN.R-  
1110 project.org/package=RColorBrewer](https://CRAN.R-project.org/package=RColorBrewer)).

1111 52. Garnier, Simon, Ross, Noam, Rudis, Robert, Camargo, A. Pedro,  
1112 Sciaini, Marco, Scherer, Cédric, *viridis - Colorblind-Friendly*  
1113 *Color Maps for R* (2021), , doi:10.5281/zenodo.4679424.

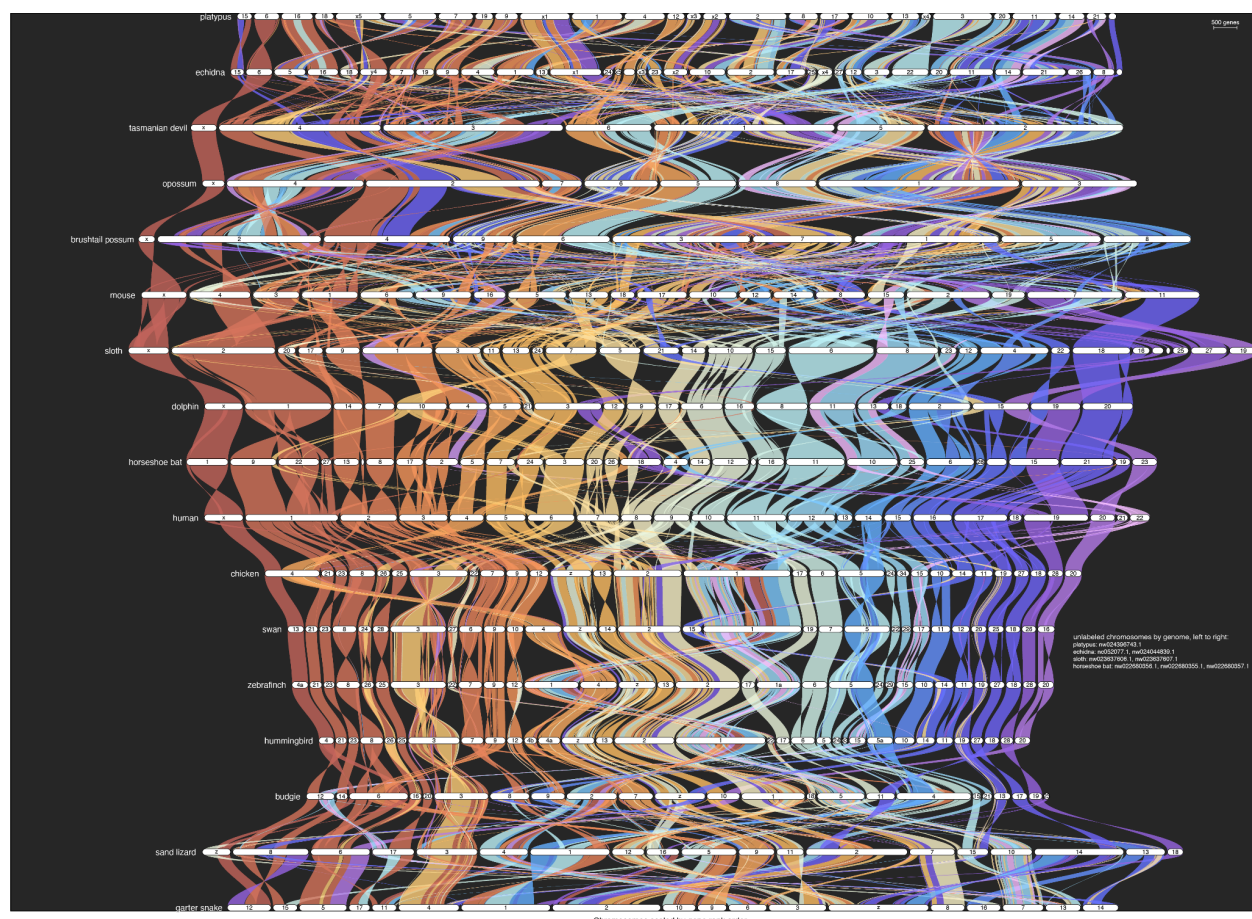
## SUPPLEMENTAL FIGURES



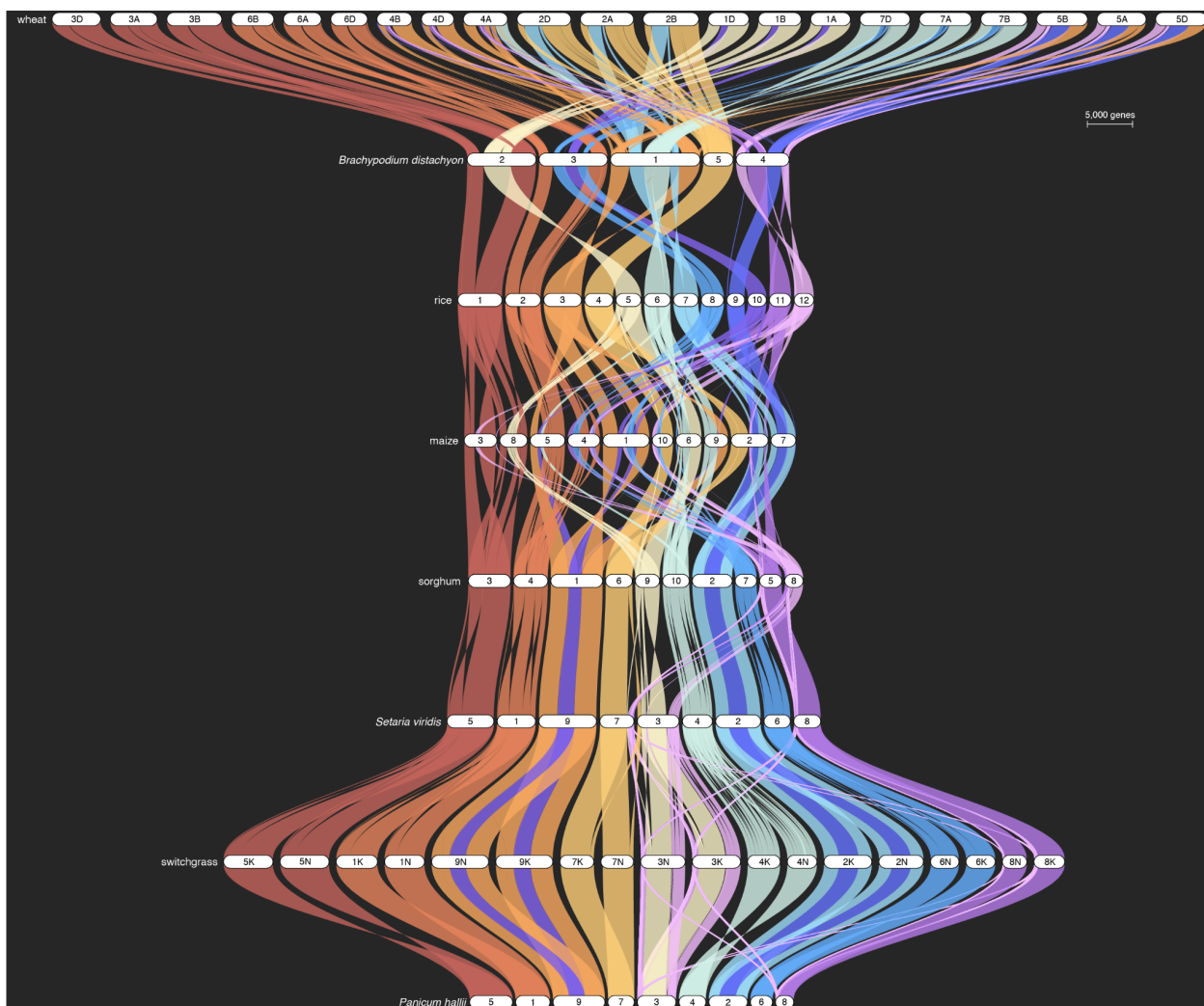
**Supplemental Figure 1 | Description of the pipeline.** Green boxes show the primary (a), synteny (b) and syntenic orthogroup (c) modules. Verbal descriptions of the three main GENESPACE functions are presented in the bottom right.



**Supplemental Figure 2 | Cotton sub-genome synteny.** The synteny map for the split-sub-genome run is presented here. The two *G. barbadense* sub-genome chromosomes are labeled; the top three A sub-genome and bottom three D sub-genome chromosomes map to these. Synteny braids are colored following the D sub-genome chromosome order.

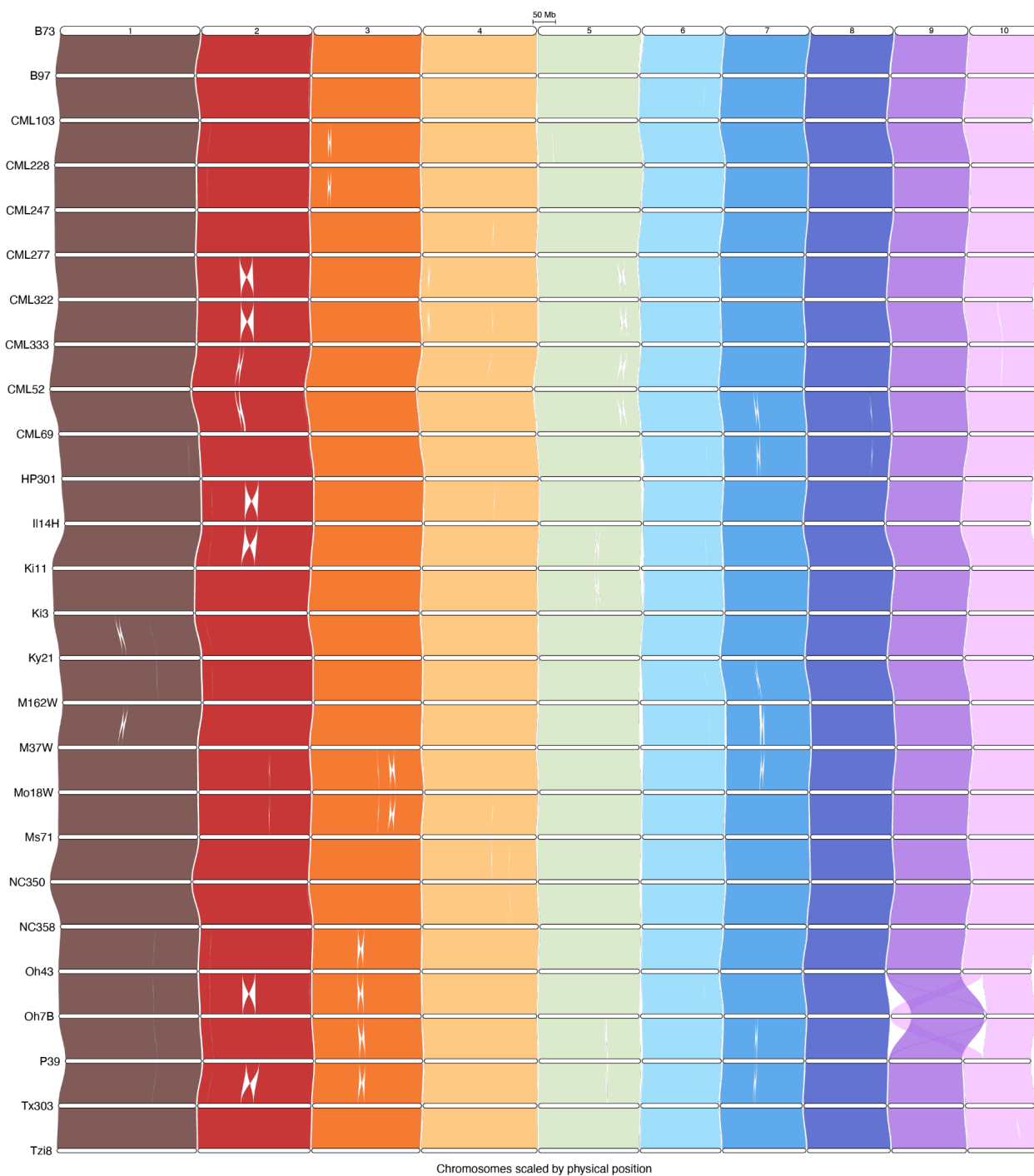


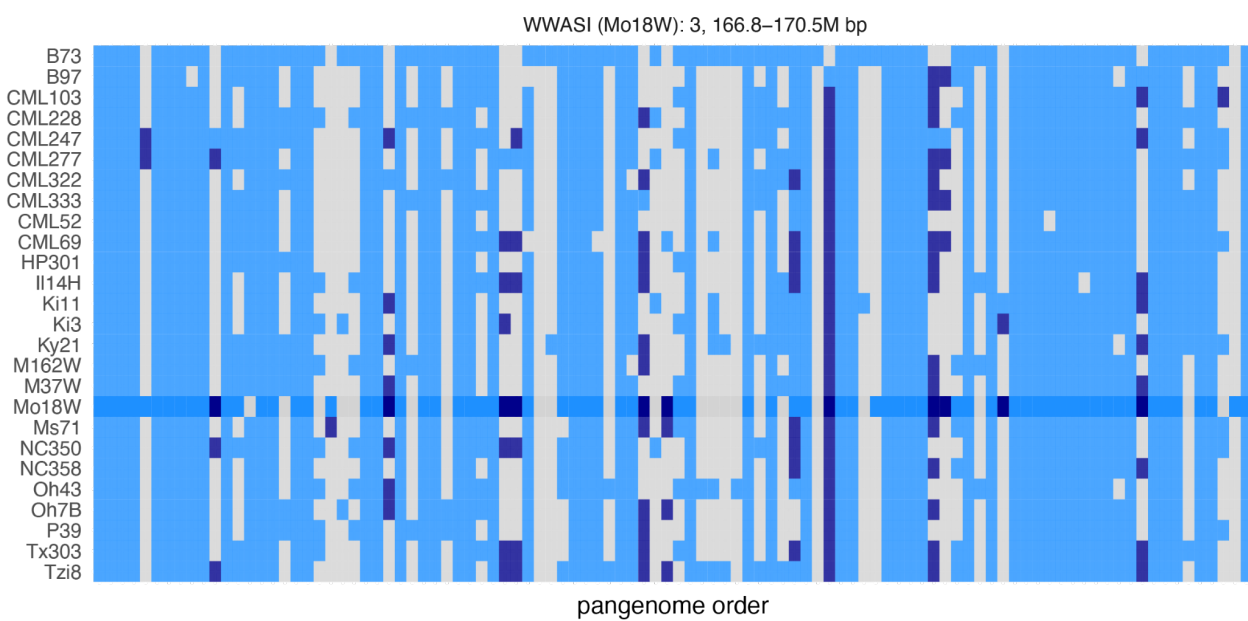
18  
19  
20  
21  
22  
**Supplemental Figure 3 | The full synteny map across 17 vertebrate genomes.** Chromosomes are ordered to maximize synteny with human chromosomes [X, Y, 1-22]. Syntenic braids are color coded by their mapping to the human chromosomes. A few scaffolds were too small for an informative label. These are listed on the right. Chromosome sizes are scaled by the number of genes with syntenic mappings to other genomes.



23  
24  
25  
26  
27  
28

**Supplemental Figure 4 | The full synteny map across 8 grass genomes.** Chromosomes are ordered to maximize synteny with rice chromosomes [1-12]. Syntenic braids are color coded by their mapping to the rice chromosomes. Chromosome sizes are scaled by the number of genes with syntenic mappings to other genomes.





**Supplemental Figure 6 | Map of presence absence variation in the larger chromosome 3 QTL interval.** Genome labels (y-axis) follow the order of other plots. Pan-genome entries are ordered by physical position within the interval on the x-axis. Gray panes are absences, dark blue are multi-copy and light blue are single-copy genes in each entry-by-genome combination. The more saturated colors correspond to the Mo18W genome, which has an outlier effect on this interval.